

CD166 MODULATES DISEASE PROGRESSION AND
OSTEOLYTIC DISEASE IN MULTIPLE MYELOMA

Linlin Xu

Submitted to the faculty of the University Graduate School
in partial fulfillment of the requirements

for the degree

Doctor of Philosophy

in the Department of Microbiology and Immunology

Indiana University

June 2016

Accepted by the Graduate Faculty, Indiana University, in partial fulfillment of the requirements for the degree of Doctor of Philosophy.

Edward F. Srour, Ph.D., Chair

Laura Haneline, M.D.

Doctoral Committee

March 16, 2016

Melissa A. Kacena, Ph.D.

Louis Pelus, Ph.D.

Attaya Suvannasankha, M.D.

Acknowledgements

I would first like to express my sincere gratitude to my mentor, Dr. Edward F. Srour, who gave me the freedom and patience to explore on my own and also the guidance and support when my steps faltered. Dr. Srour taught me how to do research and express ideas. I gained an enormous amount of priceless knowledge from him and I am truly grateful for him being my mentor during my graduate school.

Thanks my committee members, Dr. Louis Pelus, Dr. Melissa Kacena, Dr. Lauren Haneline, Dr. Attaya Suvannasankha and Dr. Angelo Cardoso for always providing me with valuable suggestions and guidance at each committee meeting. A special thanks to Dr. Khalid Mohammad, who lent his hand to me when I needed a helping hand. I am deeply grateful for his insightful comments and criticisms of my research.

Thanks also go to my former and present lab members including Brad Poteat, and BR Chitteti, who have always been willing to lend a helpful hand. I also want to thank Colin Crean, Dan Zhou and Judy Anderson. This work could not be completed without their help. Special tThanks IU Simon Cancer Center for the funding support.

Finally, I would like to thank my family for giving me support and encouragement needed through my graduate study. I thank my husband, Hao Wu and my baby, William Wu. They are always cheering me up and standing beside me through good and bad. They are the best in life.

Linlin Xu

CD166 MODULATES DISEASE PROGRESSION AND OSTEOLYTIC DISEASE IN MULTIPLE MYELOMA

Multiple myeloma (MM) is an incurable malignancy characterized by the proliferation of neoplastic plasma cells in the bone marrow (BM) and by multiple osteolytic lesions throughout the skeleton. We previously reported that CD166 is a functional molecule on normal hematopoietic stem cells (HSC) that plays a critical role in HSC homing and engraftment, suggesting that CD166 is involved in HSC trafficking and lodgment. CD166, a member of the immunoglobulin superfamily capable of mediating homophilic interactions, has been shown to enhance metastasis and invasion in several tumors. However, whether CD166 is involved in MM and plays a role in MM progression has not been addressed. We demonstrated that a fraction of all human MM cell lines tested and MM patients' BM CD138+ cells express CD166. Additionally, CD166+ cells preferentially home to the BM of NSG mice. Knocking-down (KD) CD166 expression on MM cells with shRNA reduced their homing to the BM. Furthermore, in a long-term xenograft model, NSG mice inoculated with CD166KD cells showed delayed disease progression and prolonged survival compared to mice receiving mock transduced cells. To examine the potential role of CD166 in osteolytic lesions, we first used a novel Ex Vivo Organ Culture Assay (EVOCA) which creates an in vitro 3D system for the interaction of MM cells with the bone microenvironment.

EVOCA data from MM cells lines as well as from primary MM patients' CD138+ BM cells demonstrated that bone osteolytic resorption was significantly reduced when CD166 was absent on MM cells or calvarial cells. We then confirmed our ex vivo findings with intra-tibial inoculation of MM cells in vivo. Mice inoculated with CD166KD cells had significantly less osteolytic lesions. Further analysis demonstrated that CD166 expression on MM cells alters bone remodeling by inhibiting RUNX2 gene expression in osteoblast precursors and increasing RANKL to OPG ratio in osteoclast precursors. We also identified that CD166 is indispensable for osteoclastogenesis via the activation of TRAF6-dependent signaling pathways. These results suggest that CD166 directs MM cell homing to the BM and promotes MM disease progression and osteolytic disease. CD166 may serve as a therapeutic target in the treatment of MM.

Edward F. Srour, Ph.D., Chair

Table of Contents

Chapter 1. Introduction	1
Hematopoiesis – B cell development	1
General overview of multiple myeloma.....	2
Multiple myeloma and bone marrow microenvironment	6
Multiple myeloma bone disease	9
Multiple myeloma stem cell controversy	16
CD166	20
Goals of Research.....	22
Chapter 2. Expression of CD166 on MM cells and the Role of CD166 in Cell Migration to the BM	25
Introduction	25
Materials and Methods:	26
Cells, cell culture, and mice	26
MM primary BM CD138+ cell selection, flow cytometry and sorting.....	27
Transfection and infection studies.....	28
Homing assay and mice xenograft human MM model	28
Real-time PCR	29
Statistical analysis.....	30
Results	32
CD166 is expressed on MM cell lines and primary MM CD138+ cell.....	32
CD166 is important for MM cells homing to the bone marrow of NSG mice	39
Knockdown of CD166 on myeloma cells does not alter growth kinetics in vitro	44
Homing of CD166+ MM cell to the BM of NSG mice is not dependent on the expression of CXCR4.....	44
Knockdown of CD166 on myeloma cells delays disease progression in vivo and enhances survival	45

NSG mice injected with CD166KD H929 cells had significantly less bone lesions.....	46
Discussion.....	54
Chapter 3. Role of CD166 in the pathobiology of bone lytic disease in MM	56
Introduction	56
Materials and Methods.....	59
Cells, cell culture, and mice	59
MM primary BM CD138+ cell selection, flow cytometry and sorting.....	60
In Vitro osteoclast assays	61
Mice Xenograft human MM model	61
Radiography and micro-computed tomography (micro-CT)	61
Stimulation of bone marrow monocytes (BMM) with H929 cells and Western blotting	62
Real-time PCR	63
Transfection and infection studies.....	63
Statistical analysis.....	64
Results	68
CD166 is critical for the pathobiology of bone lytic disease in MM.....	68
CD166 expression on MM cells suppresses RUNX2 expression in osteoprogenitors	84
CD166 expression on MM cells increases RANKL: OPG ratio in both BMSC and cells in calvarial bone.....	84
CD166 expression on MM cells promotes osteoclast formation in vitro	85
CD166 up-regulates key signaling pathways involved in osteoclastogenesis in MM through the regulation of TRAF6.....	86
Discussion.....	99
Chapter 4. Future Directions	103
CD166 identifies MM stem cells	103
Determine with more details and particularly in the human system the role of CD166 in bone remodeling in MM.....	108
Reference	112

Curriculum Vitae

List of Tables

Chapter 1

Table 1. Paraproteins and light chains secreted by MM cell lines 5

Chapter 2

Table 2. qRT-PCR primer sequence31

Chapter 3

Table 3. qRT-PCR primer sequence64

List of Figures

Chapter 1

Figure 1. Schematic representation of MSC differentiation.....	13
Figure 2. Osteoclastogenesis	15
Figure 3. TRAF6 signaling in osteoclastogenesis.....	19
Figure 4. CD6 and CD166 interactions between cells.	20

Chapter 2

Figure 5. CD166 is expressed on both MM cell lines and MM patients’ CD138+ cells.....	34
Figure 6. The expression of other molecules on MM cells.....	36
Figure 7. CD166+ cells preferentially home to the BM of NSG mice.	38
Figure 8. CD166KD inhibits MM cells from homing to the BM	41
Figure 9. CD166KD on H929 cells does not alter cell growth kinetics.....	43
Figure 10. Homing of H929 cells to the BM is not dependent on the expression of CXCR4.....	49
Figure 11. Mice bearing CD166KD cells showed delayed disease progression and prolonged survival.....	51
Figure 12. Mice bearing CD166KD cells had significantly less bone lesions. ...	53

Chapter 3

Figure 13. Schematic representation of ex vivo organ coculture assay (EVOCA).	67
Figure 14. EVOCA assay with H929 cells.....	71

Figure 15. EVOCA assay with OPM2 cells.	73
Figure 16. Flow cytometric analysis of CD166 expression levels on 3 MM patients' CD138+ cells in EVOCA assay	75
Figure 17. EVOCA assay with patient 1 BM CD138+ cells.	77
Figure 18. EVOCA assay results with patients 2 and 3.	79
Figure 19. Absence of CD166 on MM cell leads to less bone osteolytic lesions.	81
Figure 20. BM analysis of mice intratibially inoculated with mock or CD166KD H929 cell.	83
Figure 21. RUNX2 gene expression analysis on BMSC treated with H929 cells	88
Figure 22. RANKL and OPG gene analysis on BMSC cocultured with H929 cells or OPM2 cells.....	90
Figure 23. Osteoblastic gene analysis of calvariae cocultured with H929 cells.	92
Figure 24. Osteoclast formation assay of BMM cells cocultured with mock or CD166KD H929 cells.	94
Figure 25. Absence of CD166 expression on MM cells downregulates key signaling pathways in osteoclastogenesis.	96
Figure 26. Absence of CD166 expression on MM cells NFATc1 in osteoclastogenesis.	98

Chapter 4

Figure 27. Primary MM cells and H929 share the same group of phenotypically defined putative MMSC expressing CD166 106

Figure 28. Anti-CD166 antibody inhibits MM cell growth. 111

List of Abbreviations

AA	Ascorbic Acid
ABCG	ATP-binding cassette protein
ANOVA	Analysis of variance
APC	Arachidonic Acid
ALP	alkaline phosphatase
ALCAM	Activated leukocyte cell adhesion molecule
AKT	Protein kinase B (PKB), also known as Akt
BM	Bone marrow
BMM	Bone marrow monocyte
BSA	Bovine Serum Albumin
BV/TV	Bone volume density
CCR	chemokine receptor type
CD	Cluster domain
CFU	Colony forming unit
CFSE	5-(and -6) carboxyfluorescein diacetate succinimidyl ester
CSC	Cancer stem cell
Col1a	Collagen alpha-1
CXCR	CXC chemokine receptor
Cy7	Cyanine dye 7
DNA	Deoxyribonucleic acid
DH	Diversity domain

DKK1	Dickkopf-related protein 1
EDTA	Ethylenediaminetetraacetic acid
ELISA	enzyme-linked immunosorbent assay
EVOCA	Ex vivo organ coculture assay
ERK	Extracellular signal-related kinase
FACS	Fluorescence activated cell sorting/sorter
FBS	Fetal bovine serum
FITC	Fluorescein isothiocyanate
FSC	Forward scatter
GAPDH	Glyceraldehyde-3-Phosphate Dehydrogenase
GFP	Green fluorescent protein
Gy	Grey (unit, measure of radiation exposure) (1Gy=100 rads)
H&E	Hematoxylin and eosin
HIF-1α	Hypoxia inducible factor -1 α
HSC	Hematopoietic stem cell
HRP	Horseradish peroxidase
IACUC	Institutional animal care and use committee
IL	Interleukin
Ig	Immunoglobulin
IκB	inhibitor of kappa B
IRB	Institutional review board
IP	Intraperitoneal
IV	Intravascular

IUSM	Indiana University School of Medicine
JD	Joining domain
JNK	Jun amino-terminal kinases
KD	Knockdown
KO	Knockout
MAPK	Mitogen-activated protein kinase
MACS	Magnetic-activated cell sorting
M-CSF	Macrophage colony stimulating factor
MEM	Modified essential medium
MFI	Mean fluorescence intensity
MMP-9	Matrix metalloproteinase-9
MM	Multiple myeloma
MMSC	Multiple myeloma stem cell
MK2	MAPK-activated protein kinase 2
Micro-CT	micro-computed tomography
MyoD	Myogenic gene
MSC	Mesenchymal stem cell
MIP	Macrophage inflammatory protein
NFkB	Nuclear factor kappa-light-chain-enhancer of activated B cells
NOD/SCID	Immunodeficient nonobese diabetes/severe combined immunodeficient mice
NSG	NOD/SCID IL-2 receptor gamma null mice
NFATc1	Nuclear factor of activated T-cells, cytoplasmic 1

OPN	Osteopontin
Ocn	Osteocalcin
Osx	Osterix
OPG	Osteoprotegerin
OB	Osteoblast
OC	Osteoclast
PB	Peripheral blood
PBS	Phosphate buffered saline
PE	Phycoerythrin
Pt	Patient
PI3K	Phosphoinositide-3 kinase
PKA	Protein kinase A
P/S	Penicillin and streptomycin
PPAR-γ	Peroxisome proliferator-activated receptor gamma
QRT-PCR	Quantitative reverse transcriptase polymerase chain reaction
RBC	Red blood cell
RIPA	Radioimmunoprecipitation assay buffer
RNA	Ribonucleic acid
RUNX2	Runt-related transcription factor 2
RANKL	Receptor activator of nuclear factor kappa-B ligand
RPMI1640	Roswell Park Memorial Institute medium 1640
SDS-PAGE	Sodium dodecyl sulfate polyacrylamide gel electrophoresis
SDF	Stromal cell-derived factor

SEM	Standard error of the mean
LSK	Lin-Sca-1+cKit+ cells
SSC	Side scatter
SOST	Sclerostin
SP	Side population
SOX	SRY (sex determining region Y)-boxes
TNF	Tumor necrosis factor
TRAF6	Tumor necrosis factor (TNF) receptor-associated factor 6
TGF	Transforming growth factor
VH	Variability domain
VEGF	Vascular endothelial growth factor
VLA-4	Very late antigen-4
VLA-5	Very late antigen-5
VCAM-1	Vascular cell adhesion molecule-1
WT	Wild-type

Chapter 1. Introduction

Hematopoiesis – B cell development

The development of B cells from hematopoietic precursors is a well-organized process. B cell development starts in the fetal liver during embryonic life and continues in the bone marrow throughout our lives. The first phase of B cell differentiation in the bone marrow is antigen-independent and involves progenitor B cell proliferation and V-(D)-J gene rearrangement (1,2). B cells are derived from lymphoid progenitor cells. Cytokines secreted from bone marrow stromal cells induce TdT and recombinase (RAG-1 and RAG-2) synthesis in lymphoid progenitors. The cells then undergo V_H and D_H recombination and become early pro-B cells. V_H, D_H, and J_H rearrangements of the heavy chain complete the process of the late pro-B cell stage.

When Pro-B cells express membrane μ chains with surrogate light chains, they become pre-B cells. Pre-B receptor complex also includes Ig α and Ig β signal transduction molecules, which have ITAMs (immune-receptor tyrosine activation motifs) (3) that become phosphorylated in response to antigen-BCR binding. Antigen binding stops the cells from H chain recombination and promotes them to proliferate into B cell clones with the same μ chain. After proliferation, V_L-J_L of the light chain gene segments undergo rearrangements and the cells with V_L-J_L rearrangements become immature B cells. This is a repertoire of B cell clones

with a wide range of immunoglobulin variable regions capable of recognizing different antigens (4).

The second phase of B cell development is antigen-dependent and occurs following B cell activation by antigen binding and co-stimulation. In this stage, B cells either differentiate into memory B cells or terminal and antibody-secreting plasma cells (1). Plasma cells are the final differentiation stage of B cells.

General overview of multiple myeloma

Multiple myeloma (MM) is a plasma cell malignancy. It is characterized by two main features: malignant plasma cells that infiltrate and grow in the bone marrow and development of a progressive osteolytic bone disease (5). MM is the second most frequent hematological cancer in the US with a higher incidence rate among African Americans. According to the American Cancer Society, there are around 26,000 new cases of MM and 11,000 deaths from MM in the United States each year. MM is usually diagnosed at a later stage in life predominantly among aged individuals and men are slightly more likely to get MM than women. In the US, MM is almost twice as common among African Americans as it is among whites and being overweight or obese is another risk factor for MM. Plasma cell monoclonal gammopathy of undetermined significance (MGUS) is the precondition of MM (6). MGUS has no symptoms and is usually characterized by excess paraproteins produced by plasma cells. While in MGUS, the plasma

cells is not malignant and MGUS is not associated with bone lesions. Around 20% of patients with MGUS will progress to MM throughout their lives (7).

MM is characterized by several features, including the following:

Bone disease

Up to 90% of MM patients develop bone disease and it is the most common symptom in MM. MM bone disease is caused by the increased activity of osteoclast and decreased activity of osteoblast and bone resorption also leads to the release of calcium to the blood, causing hypercalcemia and other related symptoms. Bone lesions can be evaluated by x-ray or CT scan.

Anemia

The anemia in MM results from the overgrowth of malignant cells in the BM and the inhibition of normal red blood cell proliferation.

Kidney failure

Kidney failure in MM is mainly caused by excessive immunoglobulins produced by MM cells. The hypercalcemia caused by increased bone resorption can also contribute to kidney failure.

Table 1. Paraproteins and light chains secreted by MM cell lines

Cell line	Paraprotein+ light chain
NCI-H929	IgA kappa
RPMI8226	lambda light chain
MM1.S	lambda-light chain
OPM2	IgG lambda

Infection

Infection in MM is due to the immune deficiency. Normal plasma cells that can secrete antibodies to fight infections are inhibited by the MM malignant plasma cells, which do not produce infection-fighting antibodies and thus do not protect against infections. Although much effort has been made for effective treatments and supportive care of MM, it is still incurable. Fortunately, the prognosis and survival of MM patients improved slightly over the last several decades (8). In MM, the proliferation of clonal malignant plasma cells in the bone marrow (BM) is usually accompanied by the secretion of monoclonal immunoglobulins (paraproteins) that can be detected in the serum or urine of the patients (9).

Table 1 describes the paraproteins and light chains secreted by the commonly used MM cells lines.

Different MM clones may secrete different immunoglobulins, which makes it difficult to enrich MM cells from MM patients for research in the laboratory. However, the development of flow cytometry (FC) provided more accurate and sensitive methods to examine plasma cell populations. Traditionally, FC analysis identified CD38⁺CD45^{-dim} as MM cells (10,11). However, this gating strategy greatly excludes MM cells that are CD45⁺. CD138 (sydecan-1) is a transmembrane heparin sulfate proteoglycan that is involved in several cellular functions including cell binding, cell proliferation and cell migration (12,13). Studies have shown that CD138 is expressed on plasma cells and MM neoplastic plasma cells but not on T and B cells (14). Thus CD138 is considered

as the most specific marker for plasma and neoplastic plasma cells. The advances of multi-parameter FC and monoclonal CD138 antibody made it feasible to evaluate the expressions of CD45, CD38 and CD138 on MM cells. FC analysis with 306 MM patients' BM samples showed that CD138 can be used as a selection marker of MM patients' BM plasma cells (15). Most laboratories are now applying this method to enrich MM BM cells.

While CD138 produces very good results with fresh cells, it does not work well on later processed or frozen samples due to the fact that CD138 tends to shed rapidly from the cell surface (15,16). Using computational screen for MM plasma cell markers, CD319 and CD269, both are highly and only expressed on the surface of MM plasma cells compared to any major hematopoietic cell types, have been suggested as new enrichment markers for MM patients' BM cells (17). However, nowadays, most laboratories are still using CD138 to enrich fresh MM BM cells for research purpose since it is easier to get the antibodies for CD138.

Multiple myeloma and bone marrow microenvironment

MM is a hematological malignancy with neoplastic plasma cells accumulating and proliferating in the BM. The BM microenvironment is essential for MM cell survival and growth. The BM microenvironment is a complex milieu of cells and non-cellular components that interact together to sustain normal hematopoietic stem cell (HSC) survival and the HSC pool. This microenvironment contains extracellular matrix proteins such as fibronectin and collagen and multiple types

of “stromal” cells including macrophages, fibroblasts, osteoblasts, osteoclasts, endothelial cells (EC), immune cells, and mesenchymal stem cells (MSC) in addition to HSC and hematopoietic precursors. Interactions between MM cells and the BM microenvironment enable MM cells to modulate the microenvironment and make it favorable for the maintenance of MM cell survival, growth and proliferation as well as their drug resistance(18,19).

Extracellular Matrix (ECM)

Essentially, “stromal” cells are the main source of the BM ECM, which includes fibronectin, laminins, collagens and proteoglycans. These ECM proteins participate in cell adhesion, proliferation, migration and angiogenesis which are important for tumor development. Several reports suggested the involvement of ECM proteins in tumor expansion and their drug resistance (20,21) and provides a protective microenvironment for MM cells against chemotherapy (23,24). ECM remodeling plays a key role in MM homing and progression. Metalloproteinases, a family of proteinases, can degrade the ECM proteins to help MM migration (22). Angiogenesis is also critical for MM progression (25). MM cells interact with ECM proteins and induce the production of angiogenic cytokines to further induce angiogenesis.

Cytokines and Chemokines

The growth and proliferation of MM cells are also affected by various cytokines, including interleukin 6 (IL-6), vascular endothelial growth factor (VEGF),

hepatocyte growth factor (HGF), transforming growth factor-beta (TGF- β) and other factors.

IL-6 was shown to affect the growth of MM cells and can increase the survival of MM cells by blocking apoptosis (26). VEGF is a critical cytokine that is actively involved in angiogenesis (27) and is expressed by both MM cell lines and primary MM BM cells (28). HGF is also a potent growth and survival factor for MM expressed by MM cell lines and primary MM cells (29). TGF- β can be secreted by MM cells, BM stromal cells and osteoblasts to induce the secretion of other factors and to promote osteoclastogenesis (30). Chemokines and their receptors (31) are vital in MM cell homing to the BM, growth and bone destructions. The expression of chemokine receptors such as CXCR4, CCR1, and CXCR7 in myeloma cells has been shown to be correlated with myeloma disease progression and patients' survival (32,33). The role of CXCR4 in myeloma cell homing has been well studied (34). Studies have shown that the CXCR4 inhibitor, AMD3100 can increase the sensitivity of myeloma cells to drug treatment through disrupting myeloma cells and BM microenvironment interactions (35).

Bone marrow niche cells

As a hematopoietic malignancy in the BM, the interactions between MM cells and bone marrow stromal cells are critical for MM cell survival and proliferation.

Macrophages, an abundant cellular component of the BM niche, were shown to

support MM cell growth through increasing MM cell proliferation and decreasing MM cell apoptosis (36). Furthermore, tumor-associated macrophages heavily infiltrate the BM of MM patients and the direct contact between macrophages and MM cells plays a vital role in MM drug resistance and survival (37). EC are another important component in the BM niche. Blood vessels are essential in the tumor microenvironment to facilitate tumor migration and metastasis. In MM, endothelial cells secrete chemokines to mediate the interactions between endothelial cells and MM cells and further promote MM cell proliferation (38). Endothelial cells in MM express specific antigens to participate in angiogenesis and vasculogenesis to enhance MM dissemination (39).

Multiple myeloma bone disease

Up to 90% of MM patients develop bone disease, which not only affect patients' quality of life, but also their longevity. MM bone disease is characterized by multiple osteolytic lesions throughout the skeleton, suggesting that trafficking of MM cells from the BM and lodgment of these cells at secondary sites is important for disease progression. During bone turnover, osteoblasts are responsible for the formation of new bone while osteoclasts are the cells responsible for bone resorption. Normally, bone turnover is balanced by osteoblasts and osteoclasts activities. However, in MM patients, this balance is broken by increased osteoclasts activity and decreased osteoblasts activity.

Osteoblasts are fully differentiated cells from MSC. Runt-related transcription factor 2 (RUNX2) is the key transcription factor in osteoblastogenesis. The commitment of mesenchymal stem cells to osteoblasts differentiation depends on the proper RUNX2 expression (40). RUNX2 $-/-$ mice results in the lack of a mineralized skeleton and the absence of RUNX2 functions results in bone defects (41,42). During osteoblastogenesis (Figure 1), the expression of RUNX2 closely regulates a complex gene-regulatory network (43-45); whereby the expression of Runx2 upregulates a variety of osteoblasts lineage-specific genes including *Osx* (osterix), *Ocn* (osteocalcin), and *Bsp* (bone sialoprotein), and concomitantly downregulates the expression of non-osteoblasts genes such as the adipogenic gene PPAR- γ (peroxisome proliferator-activated receptor gamma) and the myogenic gene *MyoD*. In MM, Osteoblastogenesis and osteoblasts differentiation are impaired through the downregulation of RUNX2 activity by myeloma cells (46). The downregulation of RUNX2 activity further leads to the repression of *Ocn*, *Bsp* and alkaline phosphatase (ALP) gene expression which ultimately result in suppressed bone formation in MM.

Osteoclasts are multi-nucleated cells derived from the hematopoietic monocyte-macrophage lineage. Receptor activator of nuclear factor kappa-B ligand (RANKL) and its receptor RANK are essential modulators in osteoclast maturation and activation. During normal osteoclastogenesis, RANKL, produced by osteoblasts, binds to RANK on osteoclast precursors and leads to osteoclast differentiation. Macrophage colony-stimulating factor (M-CSF), another important

cytokine secreted by osteoblasts, binds to its receptor on osteoclast precursors, and promotes osteoclast maturation (47). Osteoprotegerin (OPG) is the decoy receptor of RANKL which, upon binding to RANK alters the availability of the later to promote osteoclastogenesis. The balance between RANKL and OPG or the ratio of RANKL to OPG controls osteoclast formation and maturation (Figure 2). When this ratio is high, there is an increased osteoclastogenesis and when it is low, there is a decreased osteoclastogenesis. MM cells promote the secretion of RANKL from osteoblast and it has also been reported (48) in some cases that MM cells themselves secreted RANKL, leading to an increased RANKL to OPG ratio and resulting in the osteoclast formation.

Several signaling pathways are involved in MM induced-osteoclastogenesis. Tumor necrosis factor (TNF) receptor-associated factor 6 (TRAF6), an E3 ubiquitin ligase, is a crucial adaptor protein in the formation of osteoclast (49). TRAF6 deficient mice have defective osteoclast activity (50,51). Activation of TRAF6 by upstream signaling activates downstream signaling pathways including NFkB, PI3K/AKT and MAPK pathways (52,53). These pathways further lead to the upregulation of key modulators in osteoclastogenesis and results in osteoclast formation and differentiation (Figure 3). TRAF6 signaling has been shown to be activated in MM by several investigators (54,55), providing a therapeutic target in the treatment of MM.

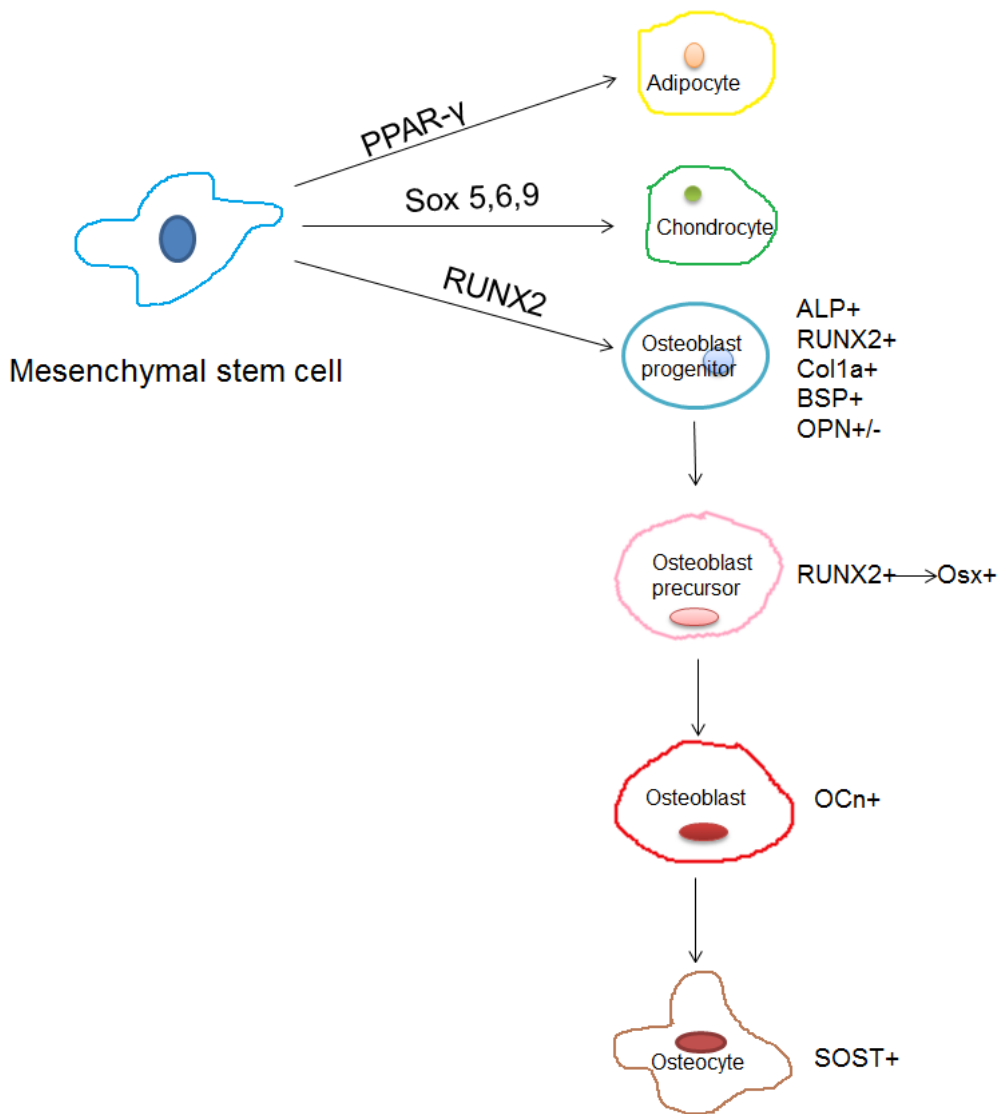


Figure 1. Schematic representation of MSC differentiation

Osteoblasts, chondrocytes and adipocytes differentiate from a common pluripotent precursor, the MSC. A number of regulators control MSC lineage fate. RUNX2 is the key transcription factor for osteoblasts differentiation.

Figure 2. Osteoclastogenesis

RANKL expressed on stromal cells or osteoblast binds to RANK on osteoclast precursors, leading to osteoclastogenesis. OPG is a decoy receptor for RANKL. The binding of OPG to RANKL blocks RANK binding, resulting in decreased osteoclastogenesis. M-CSF is also expressed by stromal cells/osteoblasts. The binding of M-CSF to its receptor c-Fms on osteoclast precursors, also leads to osteoclast differentiation.

Multiple myeloma stem cell controversy

The concept of cancer stem cells (CSC) hypothesizes that a small population of cancer cells is responsible for the initiation and proliferation of cancer (56).

Compared to normal stem cells, CSC are not only predicted to be clonogenic, but also drug resistant. CSC express proteins such as anti-alkylating enzymes like aldehyde dehydrogenase (ALDH) (57) to neutralize therapeutic drugs or members of the ATP-binding cassette (ABC) family of transporters (58) that pump the therapeutic agents out of the cells.

Despite therapeutic advances, MM remains incurable due to relapse and therapy-refractory disease. Persistence of drug-refractory MM stem cells (MMSC) provides a possible explanation for this clinical outcome. Targeting these cells is therefore appealing in MM therapy and prompted a search for MMSC. However, contradictory results about MMSC phenotype have been obtained. Studies by the group of Matsui in John Hopkins established the composite phenotype of CD45+CD34-CD138-CD38+CD19+CD27+ cells as a population enriched in MMSC (59). Essentially, a rare cell population phenotypically similar to normal memory B cells (CD20+CD27+) but lacking CD138 are the long term proliferating MM cells (60). In contrast to CD138-positive cells, CD138 negative cells could initiate tumor in NOD-SCID mice and differentiate into CD138 positive myeloma cells. Further research on these cells demonstrated that they express proteins to detoxify therapeutic drugs and efflux the drugs out of the cells. However, studies by other groups raise controversy

regarding the true nature of cells with this phenotype. Quesnel et al (61) showed, in both patients and MM cell lines, CD34⁺CD138⁺B7-H1 cells are clonogenic MM cells and MM cells with this phenotype can initiate myeloma in NOD-SCID mice. The ability to efflux Hoechst 33342 by the ATP-binding cassette protein 2 (ABCG) and/or ATP-binding cassette transporter 1 (ABCT) identifies a subset of cells from normal and malignant tissues—side population (SP) cells (62,63) which display stem cell properties. Several groups have identified SP cells in human MM cell lines and patient samples using Hoechst 33342 staining. However, Matsui and co-workers identified SP cells within the CD138⁻ MM subpopulation while Quesnel's demonstrated that the clonogenic SP cells in MM expressed CD138. Moreover, Yaccoby et al (64) using SCID mice implanted with human fetal bone fragments (SCID-hu mice), showed that CD38^{high}CD45^{neg}MM cells can repopulate in the implanted bone and self-renew in secondary SCID-hu recipient mice (65).

Due to the differences in stem cell purification protocols and mice models employed to test the properties of the putative CSC, there is a major controversy regarding the phenotype of MMSC. To definitely confirm the stemness characteristics of certain phenotype of MM populations, in vitro and in vivo assays at single cell level should be investigated.

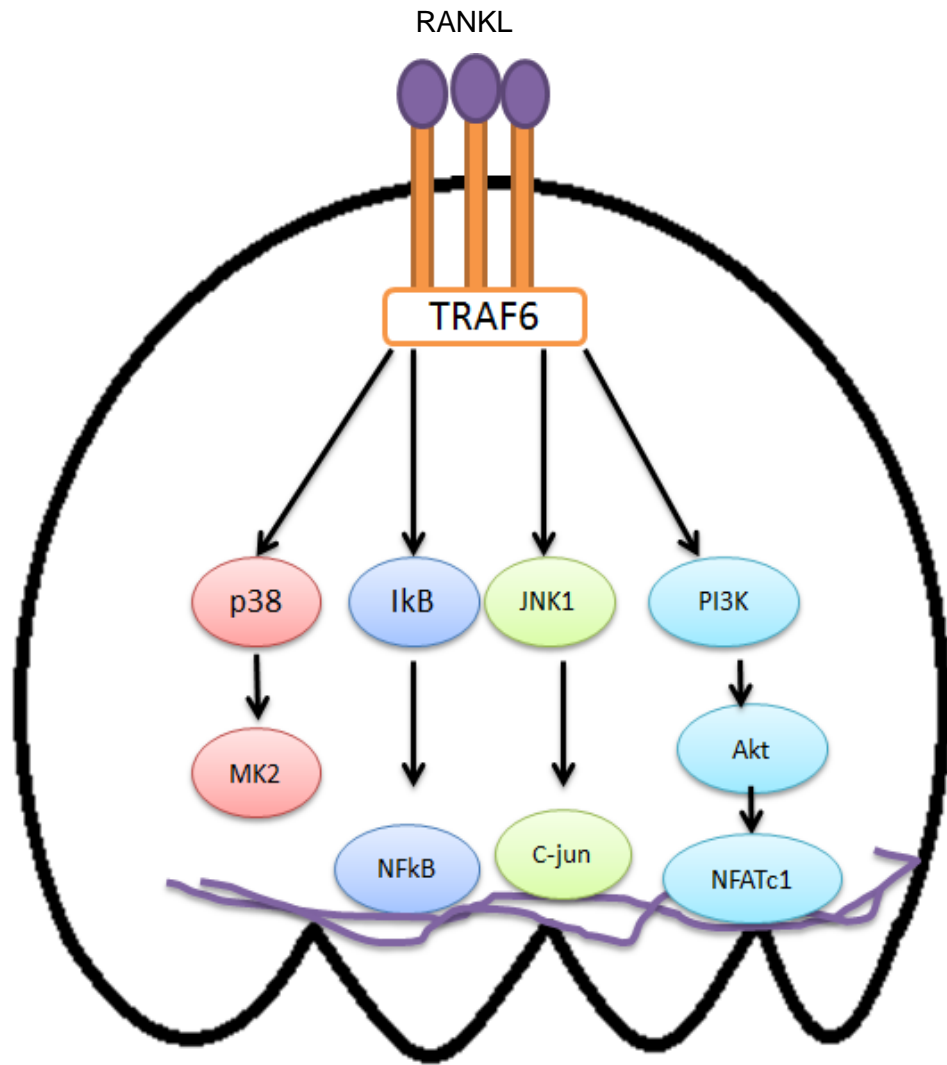


Figure 3. TRAF6 signaling in osteoclastogenesis

In osteoclast precursors, the binding of TRAF6 upstream signaling, such as RANKL to RANK, leads to the activation of TRAF6. The activation of TRAF6 leads to the activation of the downstream pathways, such as Akt, p38/MAPK and NFkB. These signals activates NFATc1, which is a key modulator in osteoclastogenesis, leading to osteoclast differentiation.

CD166

Activated leukocyte cell adhesion molecule (ALCAM/CD166) is a member of the immunoglobulin superfamily with five extracellular immunoglobulin-like domains (VVC2C2C2), a transmembrane region, and a short cytoplasmic tail. huCD166 gene was located on human chromosome 3q13.1-q13.2(66). CD166 is capable of mediating both homophilic interactions with CD166 and heterophilic interactions with CD6 (Figure 4), which is expressed on the outer membrane of T-lymphocytes and other immune cells and important for T cells activation (67,68). The CD6 binding site of CD166 is located on CD166 N-terminal domain (69) and all the residues critical for CD6 binding are conserved between human and murine CD166 demonstrated by mutagenesis studies by Bowen et al (70). As the binding of CD6, homophilic interactions of CD166 is also happening in N-terminal domain (67). There is competition between heterophilic and homophilic interaction as shown by mass spectrometry analysis(69). The expression of CD166 is conserved across species (71) with 90% homology between murine and human (70), suggesting that CD166 from both species can interact with each other and modulate cell activities from mouse or human. CD166 is involved in various physiologic and pathologic processes including cell adhesion, cell migration, and hematopoiesis and tumor progression (72,73). Recent studies demonstrated that the expression of CD166 is positively correlated with disease progression in several cancer models including breast cancer and melanoma. In breast cancer, CD166 is crucial for breast cancer cell survival by inhibition of cell death (74). In melanoma, CD166 is important for melanocytic tumor progression

and metastasis (75,76). The levels of CD166 expression on tumor cells is positively correlated with the prognosis.

CD166 has been demonstrated as a cancer stem cell (CSC) marker, including colon CSC and prostate CSC (77). In prostate cancer, CD166+ TRA-1-60+CD151+ CSCs can form spheres in vitro and initiate tumor formation in vivo. CD166 also identifies a population of multipotent colon CSC. The function of CD166 in tumors is related to adhesive properties based on homophilic interactions.

The expression of CD166 on stem/progenitor cells and its role in hematopoiesis have been described in several studies. Our laboratory has shown that CD166 is a functional marker on HSC and the expression of CD166 on HSC is critical for their homing to the BM and engraftment (78). Beside the expression of CD166 on hematopoietic stem/progenitor cells, it is also expressed on hematopoietic stem cell niche cells including MSC, osteoblast, endothelial cells (68,79), indicating that the hemophilic interactions mediated by CD166 may be essential for the maintenance of the hematopoietic stem cell pool.

How CD166 is regulated is not well known. In hepatoma cells, CD166 and miR9-1 are identified as the targets of NFκB. Under serum starvation condition, NFκB activation upregulated CD166 transcription. However, miR9-1 upregulation by NFκB was delayed, resulting in the repression of CD166 translation through its

target sites in the 3'-UTR of CD166 mRNA, forming a negative regulatory loop downstream of NFkB (80). Gilsanz et al (81) reported that the tetraspanin CD9 can augment CD166 clustering and upregulate CD166 surface expression to promote CD166 adhesive function.

Goals of Research

While the role CD166 plays in hematopoiesis has been extensively studied, it is only in the last few years that researchers have begun to appreciate the role of CD166 in cancer and cancer stem cells. Many groups around the world have investigated the function of CD166 in various cancer models, including breast cancer and melanoma. However, the role of CD166 in MM has not been investigated. We previously demonstrated that CD166 plays an important role in sustaining the ability of osteoblasts to support the maintenance and function of HSC. We also recently reported that CD166 is an important molecule on normal murine and human HSC and is critical for HSC homing to the BM and engraftment. Interestingly, our studies demonstrated that CD166 is a functional marker on normal HSC and osteoblasts since CD166- HSC engrafted poorly in normal hosts and the microenvironment of CD166- KO mice did not support the long-term engraftment of normal HSC. Taken together, these data prompted us to investigate whether CD166 is involved in the trafficking of MM cells or in modulating MM disease progression and osteolytic diseases.

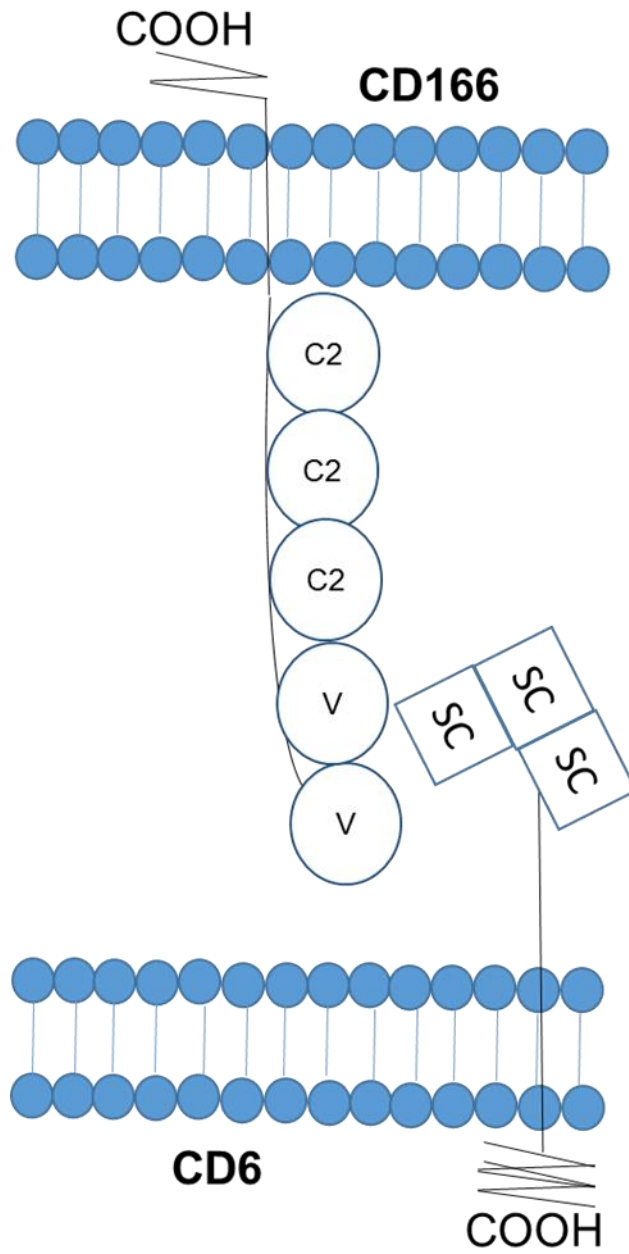


Figure 4. CD166-CD6 interactions between cells

CD6 contains three SRCR domains (Sc, squares) and CD166 contains five IgSF domains (two V and three C2). The membrane proximal domain of CD6 binds the N-terminal immunoglobulin superfamily (IgSF) domain of CD166.

Chapter 2. Expression of CD166 on MM cells and the Role of CD166 in Cell Migration to the BM

Introduction

CD166 is a member of the immunoglobulin superfamily that mediates both heterophilic CD6-CD166 and homophilic CD166-CD166 interactions. The amino acid sequences of human CD166 (huCD166) and murine CD166 (mCD166) display an overall identity of 93% (70). Besides being involved in multiple biological processes, CD166 is overexpressed in various tumor models, such as invasive melanoma, breast cancer and prostate carcinoma, and is an independent prognostic marker for several cancers (82). However, whether or not CD166 is involved in myeloma disease progression has not been investigated.

Myeloma is characterized by multiple lytic lesions throughout the skeleton. Studies also show that MM cells can be detected in the PB (83). These observations indicate that MM cells may disperse from their place of origin and cause osteolytic lesions at multiple sites throughout the skeleton, and MM cells have the capacity to traffic from BM to the PB and (re)lodge at secondary sites in the BM (homing). Similar to the migration and homing process of normal leukocytes, BM homing of MM cells is mediated by multiple adhesion molecules through a multistep process. Although several studies have investigated the mechanisms of MM homing (84,85), mechanisms of trafficking and homing of

MM cells into the BM microenvironment and MM pathogenesis have not been well understood.

As an adhesion molecule, CD166 has been shown to be involved in metastasis in several cancer models, including breast cancer and melanoma (74-76). We have recently reported that CD166 is an important molecule on normal HSC from murine and human hematopoietic tissues and plays a critical role in HSC homing to the BM and engraftment (78,86). In this chapter, we first examined the expression of CD166 on MM cell lines and MM patient cells. Then we assayed whether or not CD166 is involved in MM homing and disease progression.

Materials and Methods

Cells, cell culture, and mice

The H929 and RPMI 8226 human MM cell lines were purchased from ATCC. The OPM2 and JJN3 cell lines were generously provided by Dr. G. David Roodman (IUSM, Indianapolis, IN). CD138-positive primary myeloma cells from patients were kindly provided by Drs. Attaya Suvannasankha and Rebecca Silbermann (IUSM, Indianapolis, IN). MM cells were cultured in RPMI 1640 and were supplemented with 10% fetal bovine serum (FBS) and 1% penicillin and streptomycin (P/S). All cells were maintained at 37 °C with 5% CO₂ air. All studies using human cells were approved by the institutional review board of the IUSM.

Adult NOD.Cg-Prkdcscid Il2rgtm1Wjl/SzJ (NSG) mice (6- to 8-week-old), C57BL/6 mice and ALCAM^{-/-} (CD166^{-/-}) mice (6- to 8-week-old or 10-day old pups) were used. Mice were bred and housed in the animal facility at Indiana University. For MM inoculation studies, NSG mice received 275 cGy ionizing radiation from a cesium source followed by cell inoculation approximately 2 h later. All procedures were approved by the Institutional Animal Care and Use Committee of the IUSM and followed National Institutes of Health guidelines.

MM primary BM CD138+ cell selection, flow cytometry and sorting

MM primary BM CD138⁺ cells were selected by immunomagnetic separation (magnetic activated cell sorting, MACS) using anti-CD138 MicroBeads (Miltenyi Biotec). Briefly, MM patients' BM mononuclear cells were enriched using Ficoll-Paque Premium 1.084 (GE health care). Mononuclear cells were counted and incubated with anti-CD138 Microbeads at 10ul microbeads/ 1×10^7 cells followed by magnetic separation.

BM cell suspensions or MM cell lines were labeled with monoclonal CD166-PE antibody (Biolegend). Cells were acquired on an LSRII (BD Biosciences) flow cytometer, and events ($0.1-2 \times 10^6$) were collected and analyzed with FlowJo. CD166⁺ and CD166⁻ cells were sorted on the BD FACSAria cell sorter from MM cell lines and patient CD138⁺ MM cells after staining with anti-human CD166-PE.

Transfection and infection studies

The lentiviral vectors (pLKO1 vector with hCD166shRNA construct) to knockdown (KD) CD166 expression in MM cells was graciously provided by Dr. Helmut Hanenberg (IUSM, Indianapolis, IN).

To generate lentiviral stocks, lentiviral vectors were transfected into the packaging cell line 293T using lipofectamine 2000 (invitrogen) according to the manufacturer's instructions. Viral supernatant was collected 48 h after transfection. H929 cells were incubated with viral supernatant for 12 h and then cultured in fresh RPMI1640 at 37°C in 5% CO₂ air for 72 h. GFP-positive cells were sorted on a BD FACSAria cell sorter.

Homing assay and mice xenograft human MM model

Homing of inoculated MM cells to the BM of irradiated recipients was performed as previously described (87-89). Briefly, 2×10^7 H929-GFP (mock control or CD166KD) cells were washed with PBS and IV injected into sub-lethally irradiated NSG mice. Recipient mice were killed 14 h post-transplantation, and BM cells were recovered and analyzed for GFP-positive cells.

For mice xenograft human MM model, 200ul containing 1×10^5 H929-GFP cells (mock control or CD166KD) were IV injected into sub-lethally irradiated NSG mice. To evaluate disease progression, blood was drawn from individual mice

every two weeks until 16 weeks and human IgA (hulgA)-kappa levels were assayed in the serum with ELISA. Mouse survival was monitored over a period of 220 days. In a separate similar experiment with 14 mice/group, 6 mice from each group were euthanized at 8 weeks post-transplantation and the calvariae were dissected and processed for histology analysis. The other mice were monitored for the survival.

Similarly, NSG mice were IV injected with flow sorted CD166+ or CD166- H929-GFP/luciferase cells. After 12 weeks, mice were injected with D-Luciferin (Promega, 150mg/Kg mouse) sub-cutaneously and imaged with Berthold NightOWL LB 971 in vivo Imaging System (IUSM).

Real-time PCR

Total mRNA was extracted using RNeasy or QIAzol (QIAGEN) per the manufacturer's protocol and reverse-transcribed using SuperScript II (Invitrogen). Quantitative PCR was performed on an ABI7900 using a SYBR Green PCR Core Kit (Applied Biosystems). The primers used for quantitative PCR are listed in Table 2. Relative expression was calculated using the comparative $2^{-\Delta\Delta C_t}$ method, with GAPDH as the internal control.

Statistical analysis

Each experiment was repeated at least 3 times, and all quantitative data are presented as mean \pm SEM unless otherwise stated. Statistical differences were determined by Student t-test, log-rank test, one-way Analysis of variance(ANOVA) or two-way ANOVA with Bonferroni post t-test. Results were considered significantly different for $p < .05$.

Table 2. qRT-PCR primer sequences

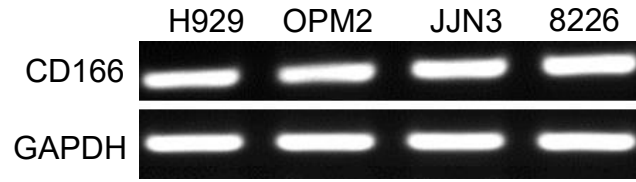
Gene Name	Forward primer sequence (5' to 3')	Reverse primer sequence (5' to 3')
Gapdh, human	AATCCCATCACCATCT TCCA	TGGACTCCACGAC GTAACA
CD166, human	CGGTCTCCTTCCAGG ATGGT	GCTTCCGTCAGCG TCAACA

Results

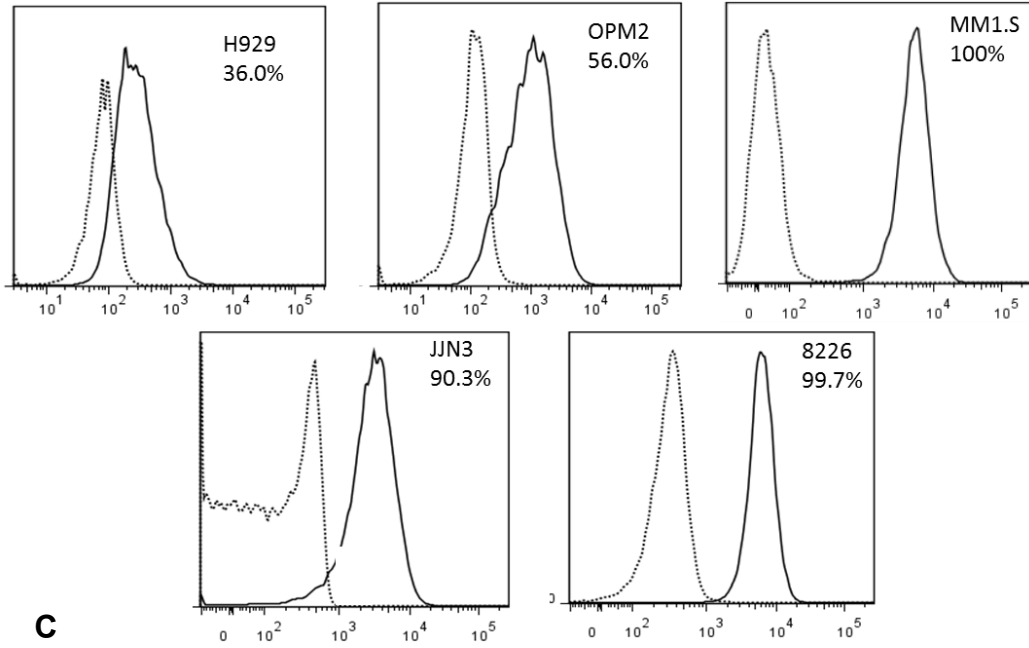
CD166 is expressed on MM cell lines and primary MM CD138+ cell

Our laboratory previously showed that CD166 is a critical functional marker on HSC (78). Since MM is a hematopoietic malignancy, we first evaluated CD166 expression on MM cells. All four cell lines tested expressed CD166 mRNA (Figure 5A). Flow cytometry also demonstrated five cell lines expressed varying levels of CD166 on the cell surface (Figure 5B). Moreover, CD166 was also expressed on CD138+ cells obtained from 6 MM patients (Figure 5C). More than 50% of CD138+ BM cells from all patients expressed CD166. However, there was no significant difference in the expression of four other markers including VLA-4, VLA-5, CXCR4 and CD90 involved in the trafficking of hematopoietic cells between CD166+ and CD166- MM cells (Figure 6A). CD6, another molecule interacting with CD166, was not expressed on MM cells including MM cell lines and MM patients' BM CD138+ cells, either (Figure 6B).

A



B



C

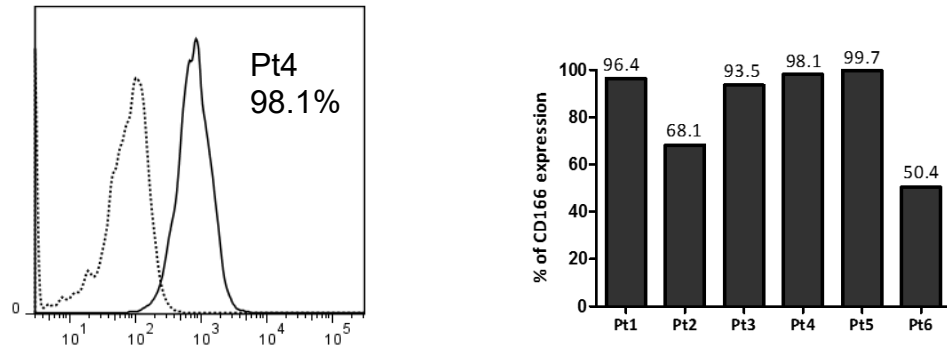
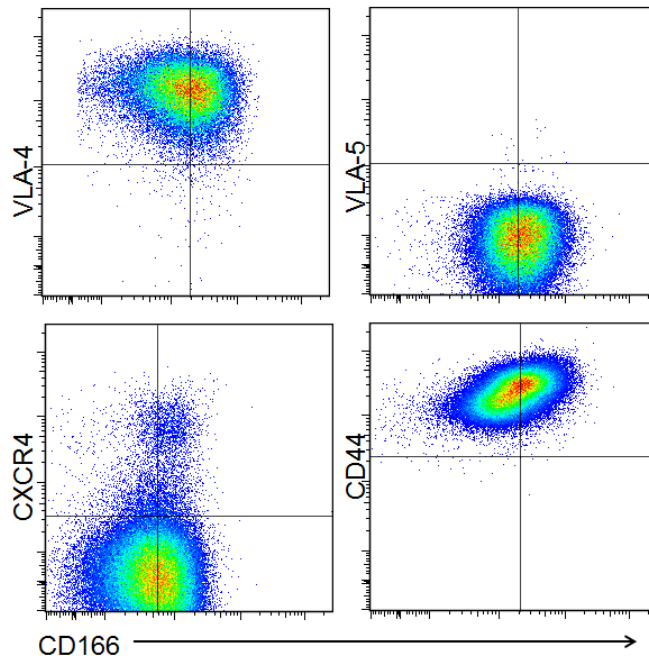


Figure 5. CD166 is expressed on both MM cell lines and MM patients'

CD138+ cells

(A) PCR analysis demonstrating CD166 expression levels on 4 MM cell lines. (B) Flow cytometric analysis of CD166 expression levels on 5 MM cell lines. (C) Left: Representative flow cytometric analysis of CD166 expression levels on MM patient' CD138+ cells. Right: CD166 expression levels on 6 MM patients' CD138+ cells. Percentage of CD166+ cells in each of the 6 samples is indicated above each bar.

A



B

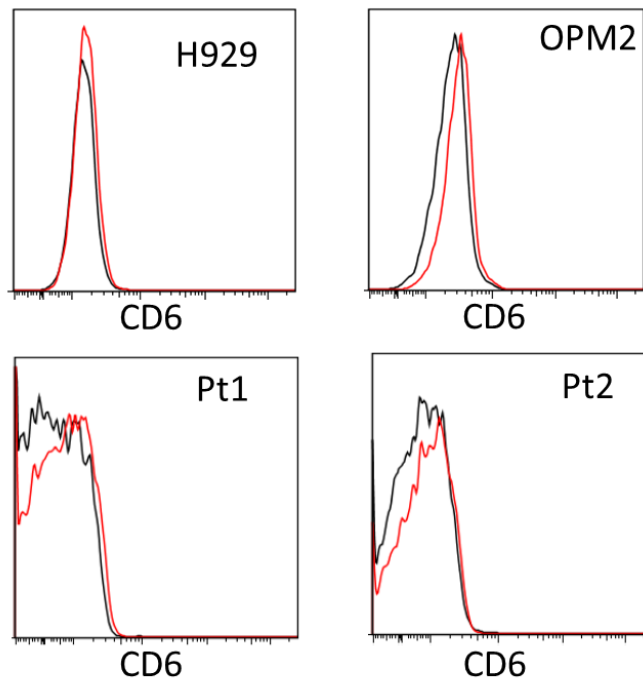


Figure 6. The expression of other molecules on MM cells

(A). Flow cytometric analysis demonstrated that both CD166+ H929 and CD166- H929 have similar expression patterns of the adhesion molecules VLA-4, VLA-5, CXCR4, and CD44. (B). Flow cytometric analysis demonstrated that MM cell lines H929 and OPM2, and two MM patient's BM CD138+ cells are negative for CD6 expression. Black line = isotype, red line = sample.

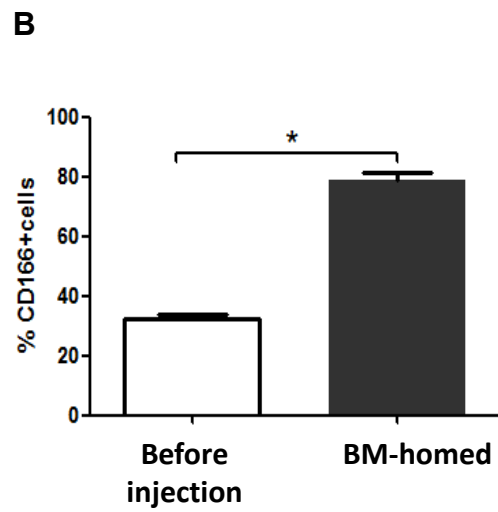
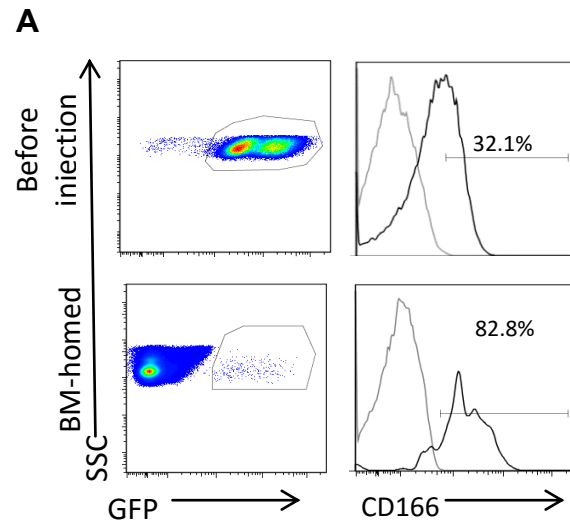


Figure 7. CD166+ cells preferentially home to the BM of NSG mice

(A-B) A total of 2×10^7 GFP-labeled H929 cells were IV injected into sub-lethally irradiated NSG mice and GFP+ cells were recovered from mice BM 14h later.

The percentage of CD166+ cells within H929 cells before injection and from BM-homed cells were compared flow cytometrically. Data are represented as mean \pm SEM from 3 pooled experiments (N = 3 mice/group/experiment, each assayed individually). Student t-test, * $p < 0.05$).

CD166 is important for MM cells homing to the bone marrow of NSG mice

We next examined the role of CD166 in the migration of MM cells to the BM using previously described homing assays (87). H929-GFP cells were injected into the tail vein of NSG mice and 14h post-injection, the mice were euthanized and the percentage of MM cells (GFP+) in the bone marrow was determined by flow cytometric analysis (Figure 7A). While the percentage of CD166+ H929 cells was originally $29.9\% \pm 1.4\%$ in H929 cells maintained in vitro, that among BM-homed cells increased to $80.0\% \pm 2.5\%$ (Figure 7B, $p < 0.05$), suggesting that CD166 facilitated or directed the homing of MM cells to the marrow microenvironment. To investigate the impact of CD166 on MM homing, we constructed GFP-tagged lentiviral shRNA for huCD166. This construct reduced the endogenous CD166 mRNA level as well as the CD166 protein level in H929 cells up to 90% (Figure 8A-B). huCD166 shRNA-expressing H929 cells displayed significantly reduced (45%) homing efficiency compared with the mock control shRNA-expressing cells (Figure 8C-D).

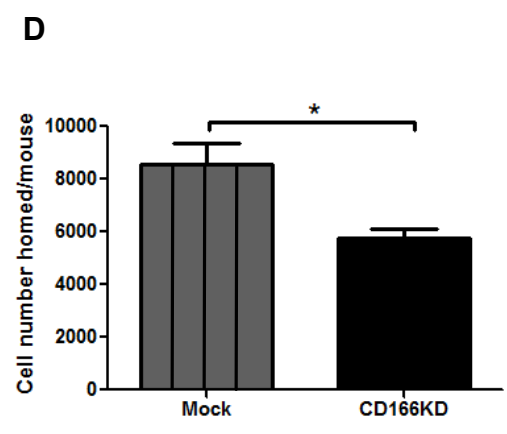
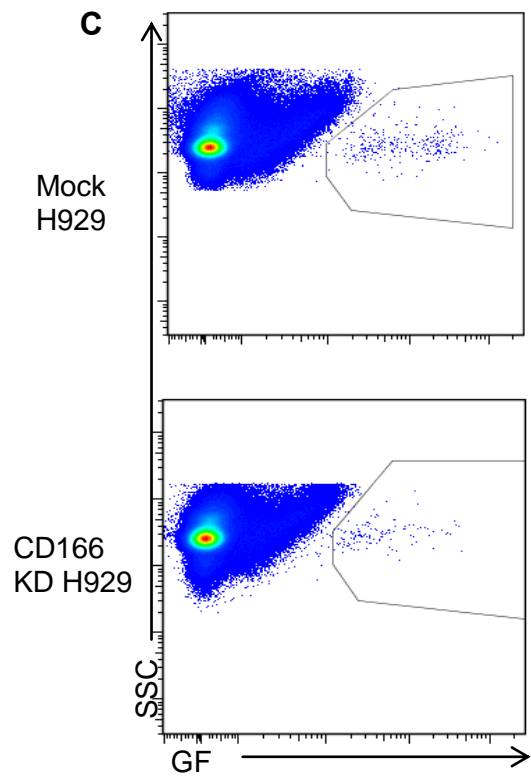
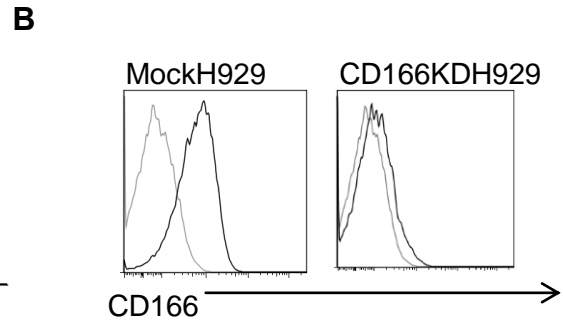
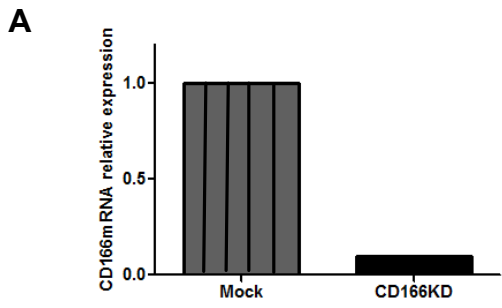


Figure 8. CD166KD inhibits MM cells from homing to the BM

(A) PCR assessment of the level of CD166 knockdown with lentiviral shRNA for huCD166. (B) Flow cytometric assessment of the level of CD166 knockdown with lentiviral shRNA for huCD166. (C) 2×10^7 GFP-labeled mock control or CD166KD H929 cells were iv injected into sub-lethally irradiated NSG mice. GFP cells were recovered from mouse BM 14h later and (D) the number of H929 cells homed to the BM was calculated. Data are represented as mean \pm SEM from 3 pooled experiments (N = 3 mice/group/experiment, each assayed individually). Student t-test, * $p < 0.05$.

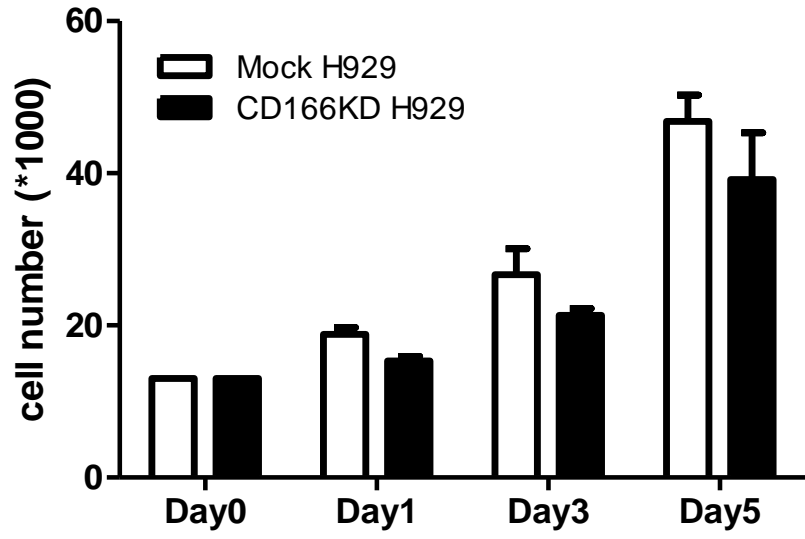


Figure 9. CD166KD on H929 cells does not alter cell growth kinetics

Mock control or CD166KD H929 cells were cultured at a density of 1.3×10^4 /ml in RPMI1640 supplemented with 1% FBS. Cell growth was examined by counting the cell number at days 1, 3 and 5. Data represent three experiments and are expressed as mean \pm SEM.

Knockdown of CD166 on myeloma cells does not alter growth kinetics in vitro

We assessed whether or not the expression of CD166 on H929 cells affects the growth kinetics of these cells. Mock or CD166KD H929 cells were seeded at a density of 1.3×10^4 /ml in RPMI1640 supplemented with 1% FBS. Cell growth was examined by counting the cell number. There is no significant difference of the growth kinetics between mock and CD166KD H929 cells (Figure 9).

Homing of CD166+ MM cell to the BM of NSG mice is not dependent on the expression of CXCR4

Previous studies by others showed that SDF-1/CXCR4 is a critical regulator of MM homing and SDF-1 dependent migration is regulated by the PI3K and ERK/MAPK pathways (84). We next examined whether or not CXCR4 is involved in CD166 mediated homing of MM cells to the BM. Using flow cytometry, we assayed the expression of CXCR4 on mock control or CD166KD H929 cells. Results from these analyses showed that there was no significant difference of CXCR4 expression levels on control H929 compare to CD166KD H929 cells (Figure 10A), indicating that CXCR4 may not participate in CD166 directed MM cell homing. We next compared the expression levels of CD166 on H929 cells in the PB to that on cells in the BM of NSG mice receiving H929 cells and found that the mean fluorescence intensity (MFI) of CD166 is significantly higher on

H929 cells in the BM compared to that in the peripheral blood (Figure 10B), indicating that CD166 is critical in directing H929 cells homing to the BM.

Knockdown of CD166 on myeloma cells delays disease progression in vivo and enhances survival

We used a xenograft model to determine the role of CD166 in initiation of MM and in disease progression. First, we investigated whether CD166 is important in initiating tumors in NSG mice. H929 GFP/luciferase cells were flow sorted into CD166+ and CD166- fractions which were then injected into NSG mice via IV injection. At 12 weeks after injection, bioluminescent imaging of the mice demonstrated a substantial difference in the tumor burden between mice with CD166+ H929 cells versus those receiving CD166- H929 cells (Figure 11A) demonstrating that CD166 contributed significantly to the burden of MM in these mice.

Using shRNA, we next examined the impact of sustained suppression of CD166 expression on the pathobiology of MM in NSG mice. NSG mice were IV injected with mock control shRNA or huCD166 shRNA-expressing H929 cells and disease progression was monitored over time. Serum levels of human IgA (hulgA) kappa in mice receiving mock control H929 were detected earlier and increased dramatically faster than in those receiving huCD166 shRNA-expressing H929 cells (Figure 11B) reflecting increased tumor burden and rapid advancement of MM in the presence of CD166. Disease progression was

monitored over a period of 220 days and survival was plotted in a Kaplan-Meier survival curve (Figure 11C). NSG mice bearing CD166KD H929 cells showed a significant delay in disease progression and prolonged survival.

NSG mice injected with CD166KD H929 cells had significantly less bone lesions

MM is characterized by multiple lytic lesions in different areas of the bone. A separate cohort of mice treated similarly with mock control or CD166KD H929 cells, was euthanized at 8 weeks post-injection to assess the severity of osteolytic lesions in these animals. Flow cytometric analysis showed that GFP-labeled H929 cells can be detected in the BM from both mice transplanted with mock or CD166KD H929 cells (Figure 12A). Radiography demonstrated significantly larger osteolytic lesion areas on the tibiae in mice inoculated with mock control cells than with CD166KD cells ($16.3 \pm 5.5 \text{ mm}^2$ vs $5 \pm 4.5 \text{ mm}^2$, $p < 0.05$) (Figure 12B). Furthermore, microCT analysis of the tibiae confirmed that these mice had significant lower trabecular bone volume (BV/TV) fraction compared to those transplanted with CD166KD H929 cells (Figure 12C). Consistent with these results, calvariae from mice receiving CD166KD cells had significantly lower osteoclast numbers per bone surface (1.6 ± 0.2) compared to those from mice injected with mock control H929 (4.4 ± 1.0 , $p < 0.05$) indicated by TRAP staining (Figure 12D-E). On the other hand, downregulation of osteocalcin mRNA, an osteoblasts differentiation marker, in calvariae was decreased when

the mice received CD166KD H929 cells (Figure 12F). These results indicate that CD166 contributes directly to the pathophysiology and progression of MM.

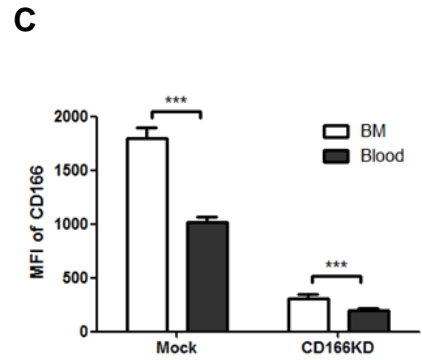
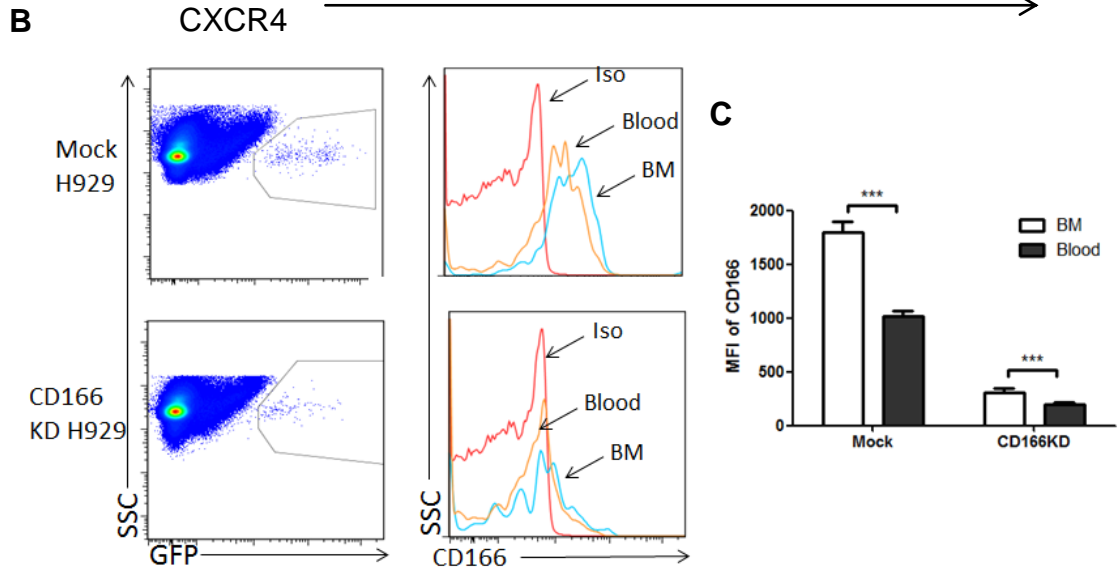
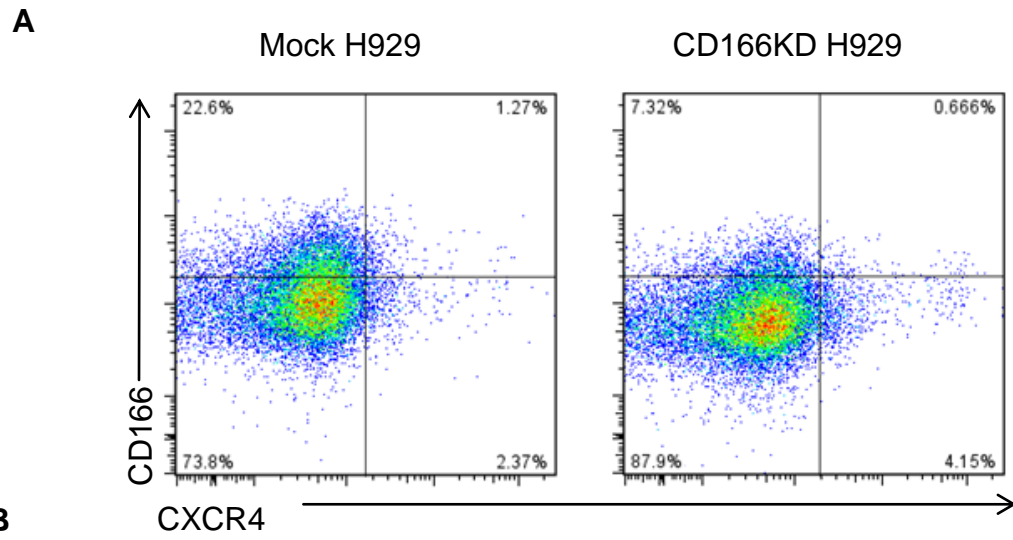
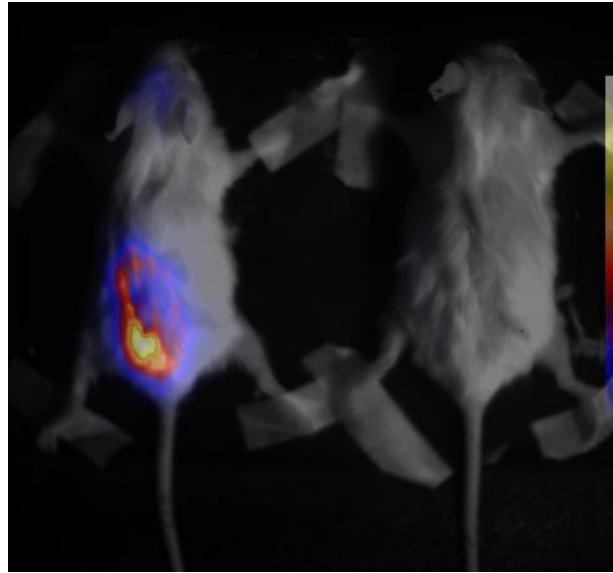


Figure 10. Homing of H929 cells to the BM is not dependent on the expression of CXCR4

(A) Flow cytometric assessment of the level of CXCR4 on mock or CD166KD H929 cells (B) 2×10^7 Mock control or CD166KD H929 cells were IV injected into NSG mice. GFP cells were recovered from mouse BM 14h later and the expression of CD166 on H929 in peripheral blood and BM were compared flow cytometrically. (C) MFI of CD166 expression on H929 cells. (N = 3 mice/group/experiment, each assayed individually). Two-way anova, ***P<0.001.

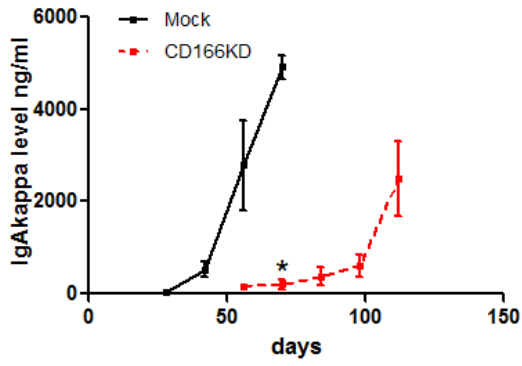
A



CD166+

CD166-

B



C

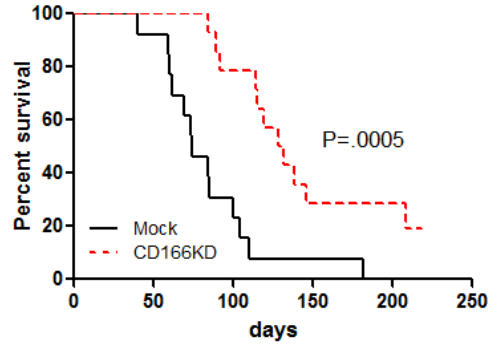


Figure 11. Mice bearing CD166KD cells showed delayed disease progression and prolonged survival

(A) 1×10^4 flow sorted CD166+ or CD166- H929 GFP/luciferase cells were injected into NSG mice. 12 weeks post-injection, the mice were injected with D-Luciferin (Promega, 150mg/Kg mouse) sub-cutaneous and imaged with Berthold NightOWL LB 971 in vivo Imaging System (IU School of Medicine) (B-C) 1×10^5 Mock control or CD166KD H929 cells were IV injected into NSG mice. (B) Human IgA-kappa levels in the serum of individual mice were measured by ELISA every two weeks. T-test, $*p < 0.05$. (C) Survival was monitored for a period of 220 days and Kaplan-Meier survival curves were plotted. Data are represented from 2 pooled experiments (N = 6-8 mice/group/experiment, each assayed individually). Long rank test, $*p < 0.05$.

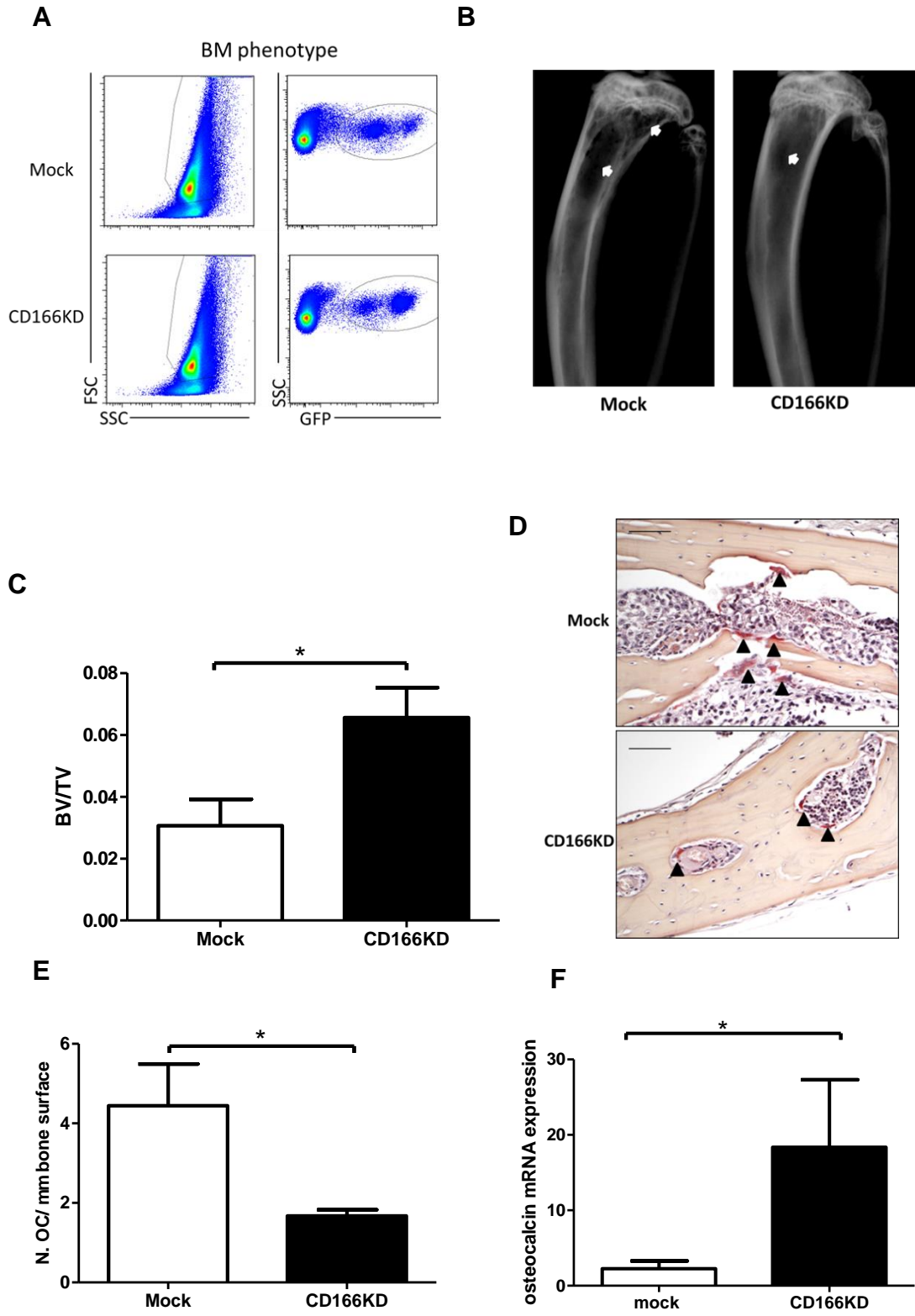


Figure 12. Mice bearing CD166KD cells had significantly less bone lesions

(A-F) 1×10^5 Mock control or CD166KD H929 cells were IV injected into NSG mice. Eight weeks after inoculation, mice were killed. (A) BM cells were flushed and GFP-labeled H929 cells were detected with flow cytometry. (B) Tibiae were imaged with radiography and representative images are shown. Bone lesions area on tibiae from mock group is bigger than those from CD166KD group (white arrow). (C) Tibiae were analyzed with micro-CT and trabecular bone volume (BV/TV) was analyzed by an analyzer blinded to the experimental groups. (D-E) Mice calvariae were fixed, decalcified and sectioned in a coronal orientation posterior to the junction of the sagittal and coronal suture and processed and stained with TRAP. (D) TRAP staining of calvariae from mice transplanted with mock control H929 cells or CD166KD H929 cells ($\times 20$, scale bar=100 μm). (E) TRAP+ osteoclasts (stained red, arrowhead) were counted from three non-overlapping fields per bone under 20 x magnifications. Data are representative of 2 separate experiments (mean \pm SEM, N = 6 mice/group/experiment, each assayed individually). Student t-test, * $p < 0.05$. (F) Expression of Osteocalcin in calvarial cells from mice transplanted with mock or CD166KD H929 cells was detected by quantitative PCR relative to GAPDH.

Discussion

Interactions between MM cells and cells of the bone marrow microenvironment are vital for MM cell growth and bone destruction (90,91). MM is characterized by multiple bone lesions along the skeleton (92), indicating that migration of MM cells from one site and lodgment in secondary sites is important for MM disease progression. In the present study, we have shown that CD166 is expressed on both MM cell lines and CD138+ primary BM cells from 4 out of 4 patients.

Our previous studies as well as early and recent studies on CD166 showed that it is expressed on cells in the bone marrow microenvironment (93,94). Using homing assays, we showed that CD166+ MM cells preferentially home to the BM while knocking down CD166 expression on MM cells impedes cell homing. Furthermore, our results indicate that CD166 is critical in directing MM cells migrating to the BM as the expression level of CXCR4, which was shown by others (84) to mediate MM cells homing the BM did not change when CD166 was knocked down in H929 cells (Figure 10A). These observations, demonstrate for the first time that CD166 is involved in MM cells trafficking and suggest that CD166 may be critical for MM pathogenesis.

To investigate the possibility of involvement of CD166 in MM pathogenesis, we investigated in a mouse model the impact of loss of CD166 expression on disease progression. To that effect, we used shRNA constructs to generate CD166KD H929 cells and established MM in cohorts of NSG mice using mock or

CD166KD H929 cells. Our data demonstrated a statistically significant difference in the survival of mice harboring mock H929 compared to those in which MM was initiated with CD166KD H929 cells. Of interest is that the osteolytic surface to bone surface ratio in mice with CD166KD H929 cells was significantly lower than that in mice with mock H929 cells suggesting the direct involvement of CD166 in MM pathogenesis and the associated bone lytic disease. These data were also confirmed by TRAP staining of calvariae and osteoclast cell counting from mice in both groups. These results suggest that the level of expression of CD166 on MM cells may be a prognostic indicator of the severity of bone lytic disease in MM. It should be noted that knocking down CD166 in H929 cells does not alter the proliferation kinetics of these cells in vitro (Figure 9) demonstrating that CD166 may not be required for the survival, proliferation, or apoptosis of these cells, but that it is critical for the interaction of MM cells with other cells in the BM microenvironment that also express CD166.

Chapter 3. Role of CD166 in the pathobiology of bone lytic disease in MM

Introduction

The BM microenvironment is crucial for MM disease progression and the associated bone lytic disease through supporting MM cell growth and expansion by increasing bone destruction through mechanisms that are not yet well-defined (91,96). Up to 90% of MM patients develop bone disease, which is associated with bone fractures, bone pain and hypercalcemia, not only affecting patients' quality of life, but also their longevity and quality of life. MM bone disease is characterized by multiple osteolytic lesions throughout the skeleton.

The basic principle of increased bone resorption in MM is unbalanced bone remodeling activity with increased bone resorption by osteoclasts and decreased bone formation by osteoblasts. MM cells suppress osteoblast differentiation and activity and stimulate osteoclast formation and function. The increased osteoclast activity further support MM cells survival and proliferation, forming a vicious circle between bone destruction and MM disease progression.

MM increases osteoclast activity

The adherence of MM cells to the BMSC, through multiple adhesion molecules and their ligands on MM cells and BMSC, leads to the upregulation of osteoclasts activating factors produced by both MM cells and BMSCs. These factors include RANKL, M-CSF, IL-6, IL-3, TNF α , TNF β , macrophage inflammatory protein

(MIP)-1 α , MIP- β , stromal-cell-derived factor (SDF)-1 α /CXCL12 (97-101).

However, investigations over the last few years have established that the RANKL and OPG system plays the most critical role in osteoclastogenesis in MM.

RANK is a transmembrane molecule belonging to the TNF receptor superfamily.

It is expressed on osteoclast precursors (102). RANKL is expressed by BMSC or osteoblasts (103). Binding to RANKL on osteoclast precursors induce osteoclast formation and maturation. RANKL is critical for osteoclastogenesis while RANKL or RANK knockout mice are deficient of osteoclasts and develop severe osteoporosis.

OPG is also a member of the TNF receptor superfamily and it is a decoy receptor of RANKL (104). OPG is expressed by osteoblasts and other cell types. The binding of OPG to RANKL inhibits RANKL interaction with RANK, thus inhibiting osteoclastogenesis. Under normal condition, the RANKL to OPG ratio is very low. However, in bone diseases, this ratio becomes either higher or lower than normal levels, leading to osteoporosis or osteopetrosis, respectively (105).

MM cells induced the increased RANKL to OPG ratio by increasing RANKL expression and decreasing OPG secretion. The increased ratio favors osteoclast formation and activity.

MM decreases osteoblast activity

The inhibition of osteoblast activity by MM is primarily mediated by direct cell-cell contact between MM cells and osteoprogenitors (46). The formation and

differentiation of osteoblasts from BMSC depends on the activity of transcription factor RUNX2. RUNX2 knockout mice lack osteoblasts or bone formation, demonstrating the critical role of RUNX2 in osteoblastogenesis (106). Coculturing human MM cells with osteoprogenitors in vitro decreased RUNX2 activity in osteoprogenitors and further inhibited osteoblast formation as evidenced by reducing the number of colony-forming units (CFU-OBs) formation and decreasing the osteoblast differentiation markers, ALP and Ocn (106). Soluble factors secreted by MM cells may also inhibit osteoblast differentiation. IL-7 has been demonstrated to inhibit RUNX2 promoter activity and IL-7 can inhibit bone formation in mice (107). Dickkopf WNT signaling pathway inhibitor 1 (DKK1) is a secreted Wnt signaling pathway inhibitor of MM cells. It is responsible for the suppression of osteoblast formation and bone destruction associated with MM (108).

In Chapter 2, we have showed that CD166 is critical for MM cells homing to the BM and MM disease progression. In this chapter, we used ex vivo culturing system and in vitro assays including ex vivo organ coculture assay to investigate whether or not CD166 is involved in MM bone diseases. Our results demonstrated that the absence of CD166 expression on MM cells diminished their ability to induce bone osteolytic lesions ex vivo and osteoclast formation in vitro. We further showed that TRAF6 signaling pathway is indispensable for CD166-induced osteoclastogenesis in MM.

Materials and Methods

Cells, cell culture, and mice

The H929 human MM cell lines were purchased from ATCC. The OPM2 cell line was generously provided by Dr. G. David Roodman (Indiana University School of Medicine, Indianapolis, IN). CD138-positive primary myeloma cells from patients were kindly provided by Drs. Attaya Suvannasankha and Rebecca Silbermann (Indiana University School of Medicine, Indianapolis, IN). MM cells were cultured in RPMI 1640 and were supplemented with 10% fetal bovine serum (FBS) and 1% penicillin and streptomycin. All cells were maintained at 37 °C with 5% CO₂ air. All studies using human cells were approved by the institutional review board of the IUSM.

NSG mice, C57BL/6 mice and ALCAM^{-/-} (CD166^{-/-}) mice (10-day old pups) were used. Mice were bred and housed in the animal facility at Indiana University. All procedures were approved by the Institutional Animal Care and Use Committee of the IUSM and followed National Institutes of Health guidelines.

For EVOCA, Calvariae from 10 day old neonatal C57BL/6 mice and global ALCAM^{-/-} mice were dissected under sterile conditions as described (109). Half of the calvariae was used to coculture with myeloma cells in a-MEM/RPMI1640 50/50 medium supplemented with 1% P/S for 10 days and the medium was changed every 72 h thereafter (Figure 13). When calvariae were cocultured with patient MM

cells, α -MEM/RPMI1640 50/50 medium with 1% P/S and 5% Bovine Serum Albumin (BSA) was used. For histology, calvariae were removed from culture and dipped in PBS then fixed with 10% neutral buffered formalin, decalcified with 10% w/v EDTA, embedded with paraffin, sectioned, and stained with hematoxylin and eosin.

MM primary BM CD138+ cell selection, flow cytometry and sorting

MM primary BM CD138+ cells were selected by immunomagnetic separation (magnetic activated cell sorting, MACS) using anti-CD138 MicroBeads (Miltenyi Biotec). Briefly, MM patients' BM mononuclear cells were enriched using Ficoll-Paque Premium 1.084 (GE health care). Mononuclear cells were counted and incubated with anti-CD138 Microbeads at 10ul microbeads/ 1×10^7 cells followed by magnetic separation.

BM cell suspensions or MM cell lines were labeled with monoclonal CD166-PE antibody (Biolegend). Cells were acquired on an LSRII (BD Biosciences) flow cytometer, and events ($0.1-2 \times 10^6$) were collected and analyzed with FlowJo. CD166+ and CD166- cells were sorted on the BD FACSAria cell sorter from MM cell lines and patient CD138+ MM cells after staining with anti-human CD166-PE.

In Vitro osteoclast assays

Primary mouse bone marrow monocytes (BMM) were used for in vitro osteoclast studies as described (110). BMM were isolated with Ficoll-Paque Premium 1.084 (GE health care) from total nonadherent bone marrow cells cultured on tissue culture dishes for 48 h. BMM were first cultured in α -MEM with 10% FBS and 1% P/S and 10ng/ml murine M-CSF (Peprotech) for 3 days and then switched to the above media with 50ng/ml murine RANKL (Biolegend) for 7 days in which mock control or CD166KD H929 cells were added to the culture at day 3. At the end of the culture, H929 cells were washed off with PBS. The adherent cells were fixed and stained with TRAP (Sigma-Aldrich). TRAP-positive cells from the whole culture in 48-well plate with 3 or more nuclei were counted as osteoclast.

Mice Xenograft human MM model

For intratibial tumor inoculation, 10ul containing 1×10^5 H929-GFP cells (mock or CD166KD) were injected into sub-lethally irradiated NSG mice under anesthesia. X-ray of the mice tibiae was performed at 4 and 8 weeks later under anesthesia. Mice were euthanized at 9 weeks. Bilateral tibiae were dissected and imaged with micro-CT. BM in the tibiae was then flushed and analyzed by flow cytometry.

Radiography and micro-computed tomography (micro-CT)

Osteolytic lesions were analyzed by radiography using a Kubtec digital X-ray imager with energy range: 10–90 kV and tube current up to 1.0 mA (Kubtec, Milford, CT). Mice were x-rayed in a prone position at 2.7x magnification. Osteolytic lesion area was measured by Bioquant image analysis software (Bioquant, Nashville, TN). Bone osteolytic lesions were quantified using a VIVACT-40 micro-CT system (Scanco Medical, Brüttisellen, Switzerland) at voxel size of 15 μm ; scanner settings: 55kVp, 145 μA and 350 ms integration time, by an observer blinded to the groups. Total bone volume was evaluated from 2mm below the most distal layer of the proximal growth plate and spanned 5 mm distally along the diaphysis. A threshold of 230 was used to manually delineate bone from surrounding soft tissue.

Stimulation of bone marrow monocytes (BMM) with H929 cells and Western blotting

BMM cells were plated in 6-well plates in α -MEM supplemented with 10% FBS and 1% P/S and 10ng/ml murine M-CSF for 3 days. The cells were then serum starved for 2 h before stimulation with mock control or CD166KD H929 cells for 30mins. H929 cells were washed off with cold PBS on ice. BMM cells were lysed with RIPA buffer (Santa Cruz Biotechnology). Total protein was extracted and the extracts were subjected to SDS-PAGE and Western blotting. Primary Abs used included TRAF6 (Biolegend), phospho-Akt, Akt, (Cell Signaling Technology), phospho-p38, p38, I κ B α , NFATc1 (Santa Cruz), actin (Sigma-Aldrich). HRP-conjugated

secondary Abs (Cell Signaling Technology) were probed and developed with ECL solution (Millipore).

Real-time PCR

Total mRNA was extracted using RNeasy or QIAzol (QIAGEN) per the manufacturer's protocol and reverse-transcribed using SuperScript II (Invitrogen). Quantitative PCR was performed on an ABI7900 using a SYBR Green PCR Core Kit (Applied Biosystems). The primers used for quantitative PCR are listed in Table 3. Relative expression was calculated using the comparative $2^{-\Delta\Delta C_t}$ method, with GAPDH as the internal control.

Transfection and infection studies

The lentiviral vectors (pLKO1 vector with hCD166shRNA construct) to knockdown (KD) CD166 expression in MM cells was graciously provided by Dr. Helmut Hanenberg (Indiana University School of Medicine, Indianapolis, IN).

To generate lentiviral stocks, lentiviral vectors were transfected into the packing cell line 293T using lipofectamine 2000 (Invitrogen) according to the manufacturer's instructions. Viral supernatant was collected 48 h after transfection. H929 cells were incubated with viral supernatant for 12 h and then cultured in fresh RPMI1640 at 37°C in 5% CO₂ air for 72 h. GFP-positive cells were sorted on a BD FACSAria cell sorter.

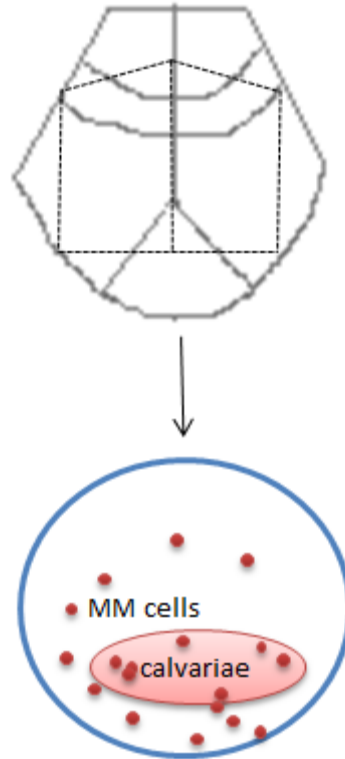
Statistical analysis

Each experiment was repeated at least 3 times, and all quantitative data are presented as mean \pm SEM unless otherwise stated. Statistical differences were determined by Student t-test, log-rank test, one-way ANOVA or two-way ANOVA with Bonferroni post t-test. Results were considered significantly different for $P < .05$.

Table 3. qRT-PCR primers sequences

Gene Name	Forward primer sequence (5' to 3')	Reverse primer sequence (5' to 3')
GAPDH,mouse	AGGAGTATATGC CCGACGTG	TCGTCCACATCCAC ACTGTT
RUNX2, mouse	CGGTCTCCTTC CAGGATGGT	GCTTCCGTCAGCGT CAACA
RANKL mouse	CATCGGGTTCC CATAAAG	GAAGCAAATGTTGG CGTA
OPG, mouse	CCGAGTGTGTG AGTGTGAGG	CCAGCTTGCACCAC TCCAA
M-CSF, mouse	TCCACCGGGAC GTAGCA	CCAGTCCAAAGTCC CCAATCT

Calvarial bone
from 10 D
Pups (WT/global CD166KO)



Cocultured for 10days, add
fresh media every 72h

Figure 13. Schematic representation of ex vivo organ coculture assay (EVOCA)

Calvariae from 10 day old neonatal C57BL/6 mice and global ALCAM^{-/-} mice were dissected under sterile conditions as described. Both halves of each calvarium were used. Each half was seeded in a cocultured system with 50,000 myeloma cells in a-MEM/RPMI1640 50/50 medium supplemented with 1% P/S for 10 days and the medium was changed every 72 h thereafter. When calvariae were cocultured with patient MM cells, a-MEM/RPMI1640 50/50 medium with 1% P/S and 5% BSA was used.

Results

CD166 is critical for the pathobiology of bone lytic disease in MM

To further investigate the impact of CD166 on osteolytic lesions associated with MM, we used an ex vivo organ culture system designed to allow for both the in vitro proliferation of MM cells including those from primary sources and for the formation of MM-associated bone lesions. Flow sorted CD166+ or CD166- H929 cells were cocultured with calvariae from 10 day-old WT or globally CD166KO pups for 10 days. At the end of the coculture, the calvariae were processed for histological analysis. Mean resorption surface to total bone surface ratio was quantified by Bioquant software. These analyses demonstrated that absence of CD166 on MM cells (CD166- H929 cells) or bone (CD166-/- calvariae) or both, significantly decreased the osteolytic lesions on the calvariae (Figure 14A-B). Similar results (Figure 15A-B) were observed when another MM cell line, OPM2 was used in similar investigations as described above.

Next, we determined whether the absence of CD166 on MM patient cells decreased bone osteolytic lesions. In a separate experiment, primary CD138+CD166+ or CD138+CD166- MM cells from three patients (Pt) were separated by flow cytometric cell sorting (the expression of CD166 on patients' CD138+ cells is shown in Figure 16) and cocultured with calvariae from 10 day-old WT or CD166 KO pups for 10 days. Similar to what we observed with MM cell lines, the lowest resorption surface to bone surface ratio was observed when

CD138+CD166- MM cells were cocultured with CD166KO calvariae (Pt1 Figure 17 and Pt2, Figure18A) or when MM cells were cocultured with CD166KO calvariae (Pt3, Figure18B).

To confirm these ex vivo observations in vivo, NSG mice were intratibially inoculated with mock or CD166KD H929 cells. Radiographic analysis revealed that mice receiving mock H929 cells developed osteolytic lesions 4 weeks after tumor inoculation. The bone deteriorated further through the course of 8 weeks. On the contrary, although tibiae from CD166KD H929 inoculated mice showed osteolytic lesions at 4 weeks, these lesions worsened to a lesser extent than that observed in the mock group over the next 4 week period (Figure 19A). In agreement, micro-CT images at 9 weeks demonstrated that mock H929 cells induced much more severe lesions in the tibiae compared to CD166KD cells (Figure 19B). Both trabecular thickness (Figure 19C) and trabecular bone volume fraction (Figure 19D) at 9 weeks post-inoculation were significantly decreased in the tibiae from mice receiving mock H929 cells. Flow cytometric analysis of the BM from the inoculated tibiae did not reveal differences in the percentage or cell number between mice inoculated with mock or CD166KD H929 cells (Figure 20A-B). However, 2 out of 5 contralateral tibiae in the mock group had detectable H929 cells (>0.1% by flow cytometric analysis). In contrast, none of the 6 contralateral tibiae of mice inoculated with CD166KD H929 cells had detectable GFP+ cells (Figure 20C). These results are consistent with our homing assay data that CD166 is critical for MM cells trafficking in the BM.

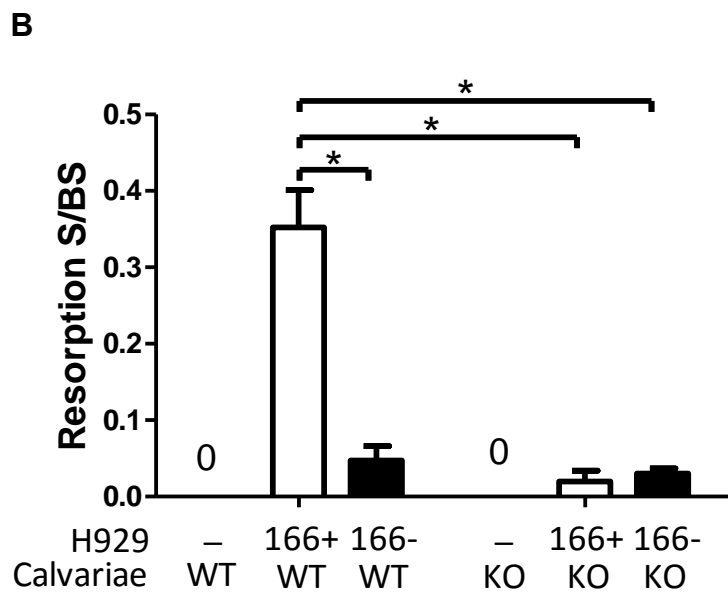
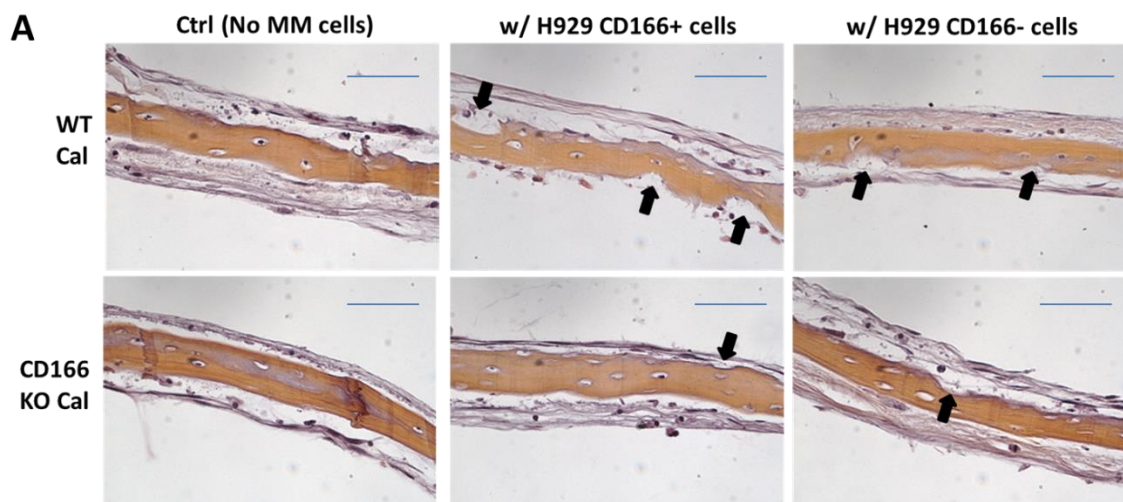
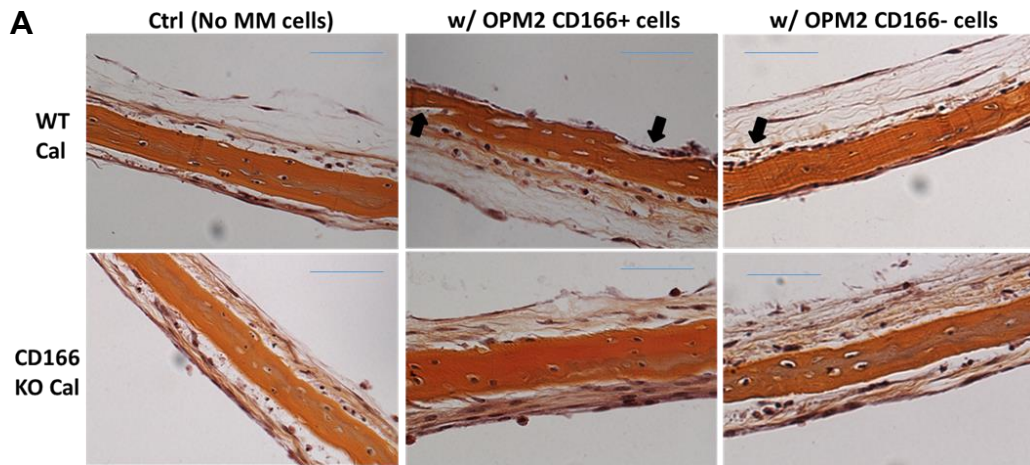


Figure 14. EVOCA assay with H929 cells

(A-B) EVOCA was used to examine the effect of CD166 expression on myeloma osteolytic lesions. Calvariae were fixed, decalcified, sectioned and processed for H&E staining. Bone resorption (black arrow) on the mice calvariae were analyzed from three non-overlapping fields per bone under 20 x magnifications. The quantitative representation of EVOCA assay was performed by measuring and calculating resorption surface to BS ratio with Bioquant software 2014. (A) H&E staining of Calvariae from WT or CD166KO pups cultured with flow sorted 2×10^4 CD166+ or CD166- H929 cells for 10 days ($\times 20$, scale bar=100 μm). (B) Quantitative representation of EVOCA assay with H929; Data represent 3 separate experiments done in triplicates for each group are expressed as mean \pm SEM, two-way anova, $*p < 0.05$.



B

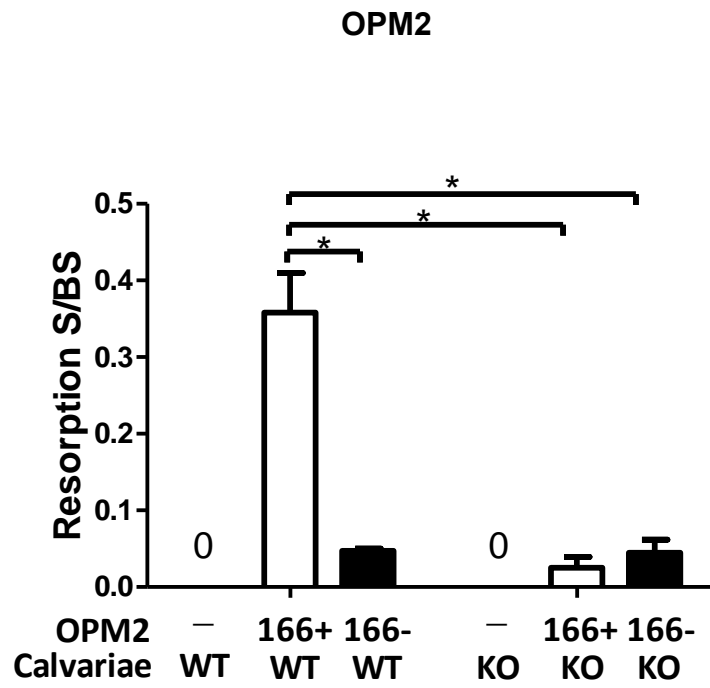


Figure 15. EVOCA assay with OPM2 cells

(A-B) EVOCA was used to examine the effect of CD166 expression on myeloma osteolytic lesions. Calvariae were fixed, decalcified, sectioned and processed for H&E staining. Bone resorption (black arrow) on the mice calvariae were analyzed from three non-overlapping fields per bone under 20 x magnifications. The quantitative representation of EVOCA assay was performed by measuring and calculating resorption surface to BS ratio with Bioquant software 2014. (A) H&E staining of Calvariae from WT or CD166KO pups cultured with flow sorted 2×10^4 CD166+ or CD166- OPM2 cells for 10 days ($\times 20$, scale bar=100 μm). (B) Quantitative representation of EVOCA assay with H929; Data represent 3 separate experiments done in triplicates for each group are expressed as mean \pm SEM, two-way anova, $*p < 0.05$.

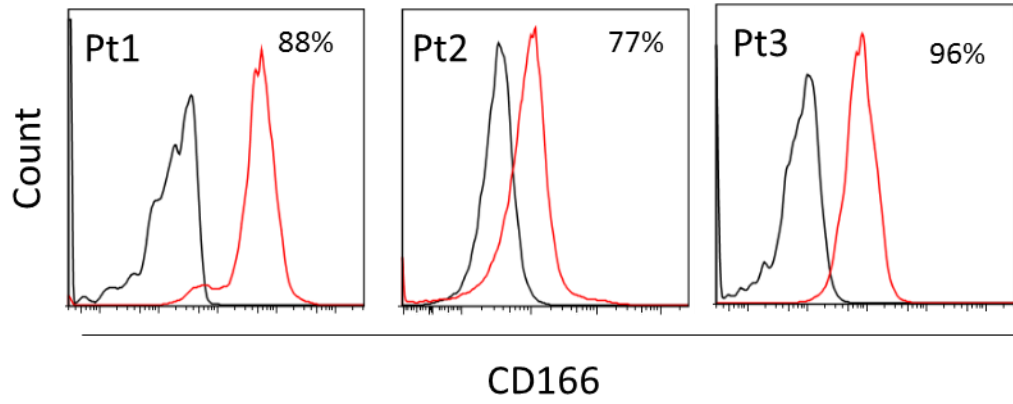


Figure 16. Flow cytometric analysis of CD166 expression levels on 3 MM patients' CD138+ cells in EVOCA assay Black line = isotype control; red line = sample

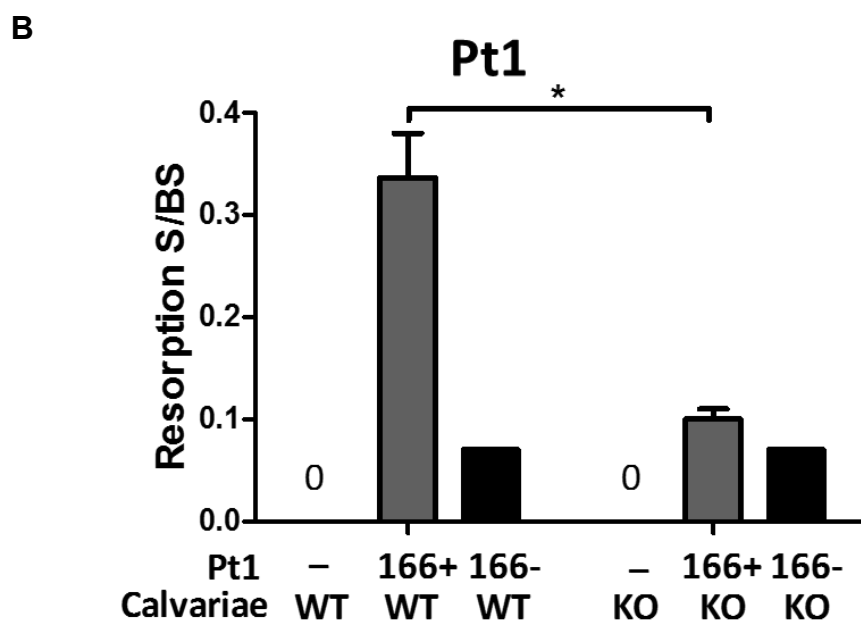
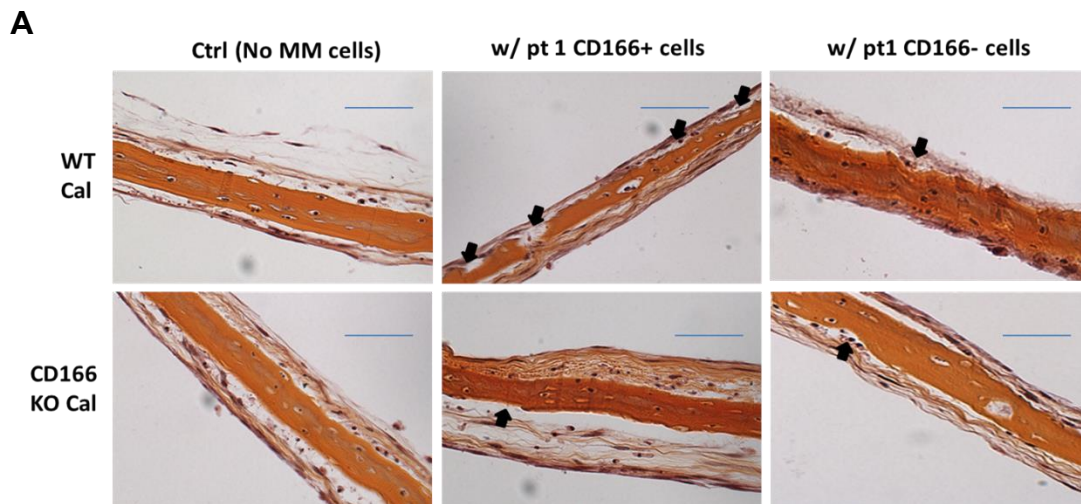
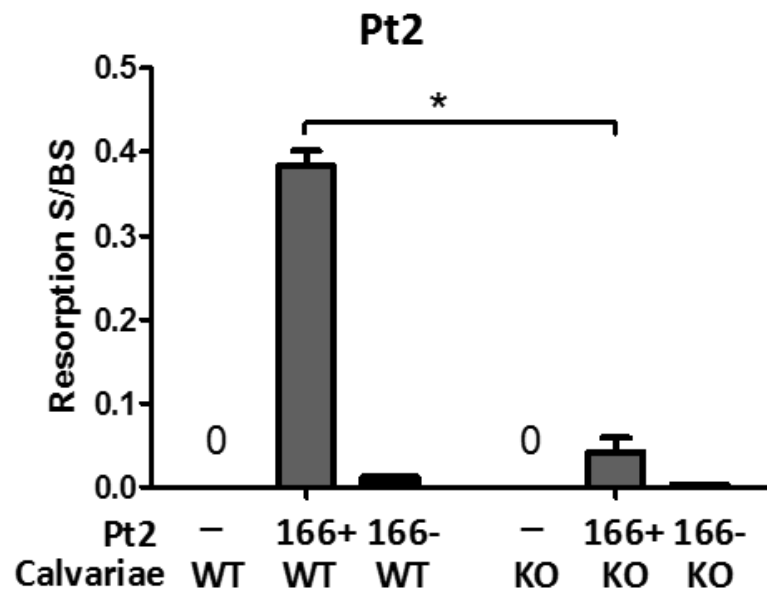


Figure 17. EVOCA assay with patient 1 BM CD138+ cells

EVOCA was used to examine the effect of CD166 expression on myeloma osteolytic lesions. Calvariae were fixed, decalcified, sectioned and processed for H&E staining. Bone lesions on the mice calvariae were analyzed from three non-overlapping fields per bone under 20 x magnification. The quantitative representation of EVOCA assay was performed by measuring and calculating resorption surface to BS ratio with Bioquant software 2014. (A) H&E staining of Calvariae from WT or CD166KO pups cultured with flow sorted 2×10^4 CD138+CD166+ or CD138+CD166- MM patient cells for 10 days. (B) Quantitative representation of EVOCA assay in (A). Two-way anova, $*p < 0.05$.

A



B

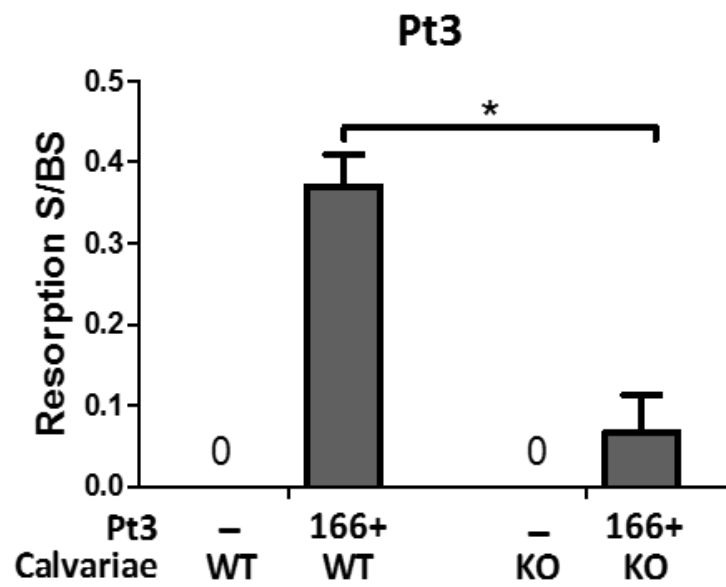


Figure 18. EVOCA assay results with patients 2 and 3

EVOCA was used to examine the effect of CD166 expression on myeloma osteolytic lesions. Calvariae were fixed, decalcified, sectioned and processed for H&E staining. Bone lesions on the mice calvariae were analyzed from three non-overlapping fields per bone under 20 x magnification. The quantitative representation of EVOCA assay was performed by measuring and calculating resorption surface to BS ratio with Bioquant software 2014. H&E staining of Calvariae from WT or CD166KO pups cultured with flow sorted 2×10^4 CD138+CD166+ or CD138+CD166- MM patient cells for 10 days. (A-B) Quantitative representation of EVOCA assay with Pt2 and Pt3 cells. Two-way anova, * $p < 0.05$.

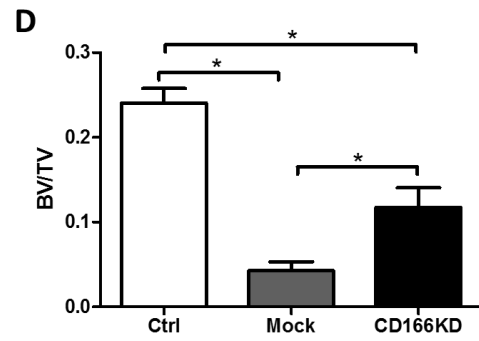
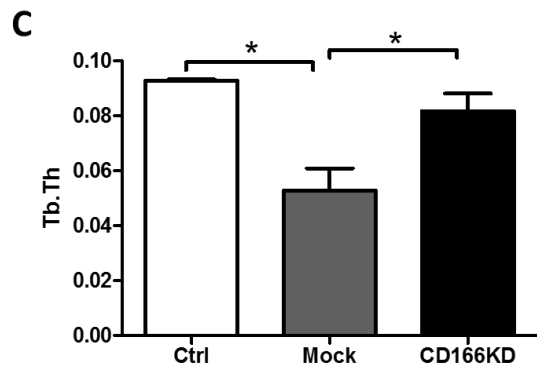
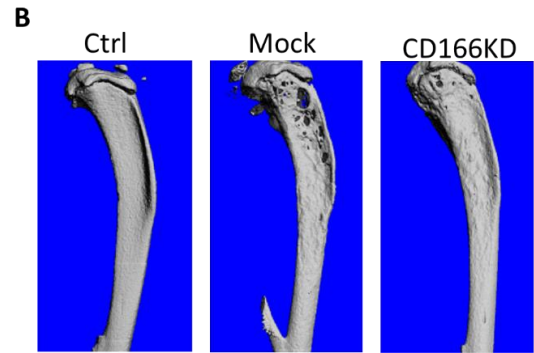
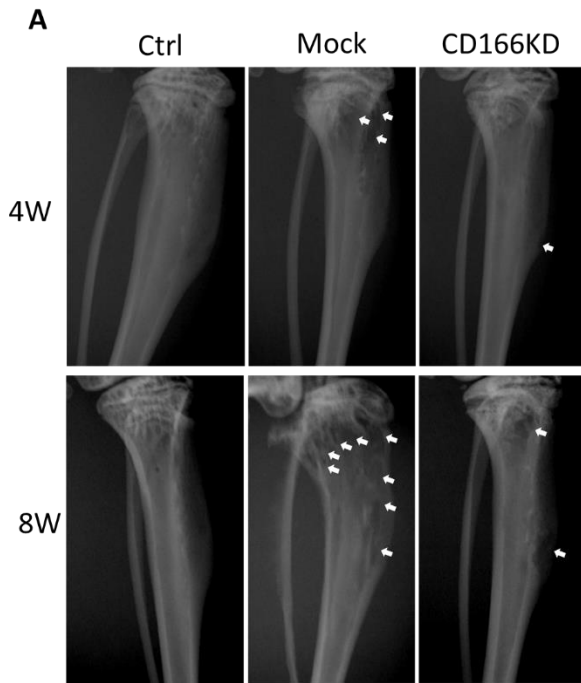


Figure 19. Absence of CD166 on MM cell leads to less bone osteolytic lesions

(A) Representative radiographic images of tibiae from mice inoculated with mock or CD166KD H929 cells at 4 weeks and 8 weeks after inoculation. Bone lesion areas are indicated with white arrow. (B) Nine weeks after inoculation, mice were euthanized and tibiae were collected and scanned using micro-computed tomography (micro-CT) for 3D reconstruction. Bones from 3 representative mice are shown. (C) Trabecular thickness Tb.Th and (D) trabecular bone volume (BV/TV fraction) were determined by micro-CT readings. n=5-6/group, mean± SEM, Two-way anova, *p<0.05.

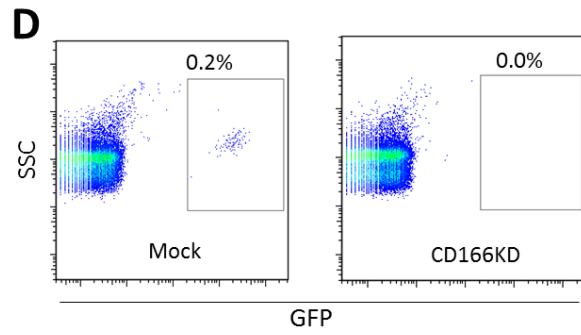
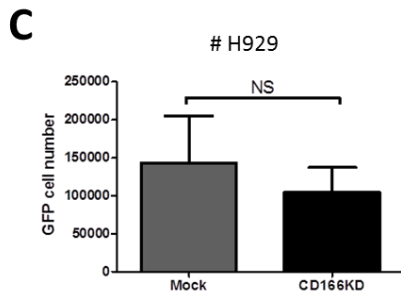
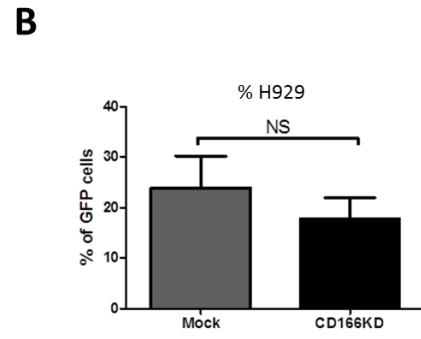
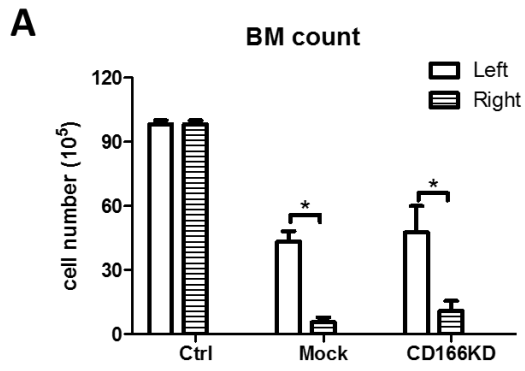


Figure 20. BM analysis of mice intratibially inoculated with mock or CD166KD H929 cell

NSG mice were inoculated with 10⁵ mock or CD166KD H929 cells in the right tibia. After 9 weeks, mice were euthanized and both tibiae were collected. After scanning both bones for micro-computed tomography for 3D reconstruction (shown in Figure 4B), BM was harvested from both tibiae and kept separate. BM counts in right and left tibiae of experimental mice and from control mice are shown in (A). (B) The percentage of GFP labeled H929 in the BM of the right tibia was analyzed with flow cytometry. (C) BM cells were counted with hemocytometer and the number of H929 cells in the right tibiae were calculated. n=5-6/group, mean± SEM, student t-test, *p<0.05, NS=no significant difference. (D) Representative flow cytometry analysis of BM from left tibiae. 2 out of 5 left tibiae from mock control group showed detectable GFP+ MM cell. However, none of the 6 left tibiae from CD166KD group analyzed by flow cytometry contained detectable (>0.1% by flow cytometric analysis) GFP+ MM cells.

CD166 expression on MM cells suppresses RUNX2 expression in osteoprogenitors

To examine how CD166 induces bone osteolytic lesions in MM, we first explored the mechanisms involved in MM-induced osteoblast suppression. BMSC were isolated from the BM of WT or CD166KO mice as described before (111) and were then cocultured with CD166KD or mock control H929 cells for 48h. H929 cells were washed off by cold PBS and RNA was isolated from BMSC. Real-time PCR results revealed that gene expression of RUNX2, a critical transcription factor in osteoblastogenesis, was significantly suppressed when CD166 was present in the culture. (Figure 21).

CD166 expression on MM cells increases RANKL: OPG ratio in both BMSC and cells in calvarial bone

We then examined the mechanisms involved in MM-induced osteoclast activation. We first measured by real-time PCR analysis gene expression levels of RANKL and OPG in BMSC isolated from the BM of WT or CD166KO mice. BMSC were then cocultured with CD166KD or mock control H929 cells for 24h. H929 cells were washed off by cold PBS and RNA was isolated from BMSC. Gene analysis showed that RANKL /OPG ratio, an important indicator for osteoclastogenic activity (112), was significantly decreased when CD166 was absent from either MM cells (CD166- H929 cells) or from BMSC cells (CD166-/-

BMSC) (Figure 22A). Similar result was observed when BMSC were cocultured with another MM cell line, OPM2 (Figure 22B).

We next measured by real-time PCR analysis gene expression levels of RANKL and OPG in calvarial cocultured with CD166KD H929 or mock control H929 cells for 7 days. At the end of the coculture, H929 cells were washed off by cold PBS and calvariae were subjected to RNA isolation. Gene analysis showed that RANKL /OPG ratio, was significantly decreased when CD166 was absent from either MM cells (CD166- H929 cells) or from bone cells (CD166^{-/-} calvariae) (Figure 23A). We also examined gene expression of M-CSF, another critical molecule on osteoclastogenesis, and found no significant difference (Figure 23B).

CD166 expression on MM cells promotes osteoclast formation in vitro

We used a previously described osteoclast differentiation assay (113) to measure osteoclastogenesis by bone marrow-derived macrophages (BMM) from WT or CD166KO mice cultured with mock control or CD166KD H929 cells. The degree to which osteoclasts were generated in culture was visibly reduced in cultures where either expression of CD166 on H929 cells was blocked or was genetically abrogated on BMM (Figure 24A). Importantly, quantification of osteoclast formation by assessing TRAP⁺ cells (≥ 3 nuclei) demonstrated that the number of TRAP⁺ cells was significantly compromised in cultures where CD166

was absent from H929 cells or when BMM were collected from CD166KO mice (Figure 24B).

CD166 up-regulates key signaling pathways involved in osteoclastogenesis in MM through the regulation of TRAF6

To further delineate the mechanisms involved in CD166-induced osteoclastogenesis in MM, we starved BMM for 2h then stimulated these cells with mock control H929 or CD166KD H929 cells for 30mins. BMM were then subjected to western blot analysis for Tumor necrosis factor (TNF) receptor associated factor 6 (TRAF6), a TNF receptor associated factor that plays a critical role in the signal transduction pathways in osteoclastogenesis (114). Our results indicate that while BMM from WT mice upregulated TRAF6 expression upon stimulation with control H929 cells, WT BMM stimulated by CD166KD H929 or BMM from CD166^{-/-} mice failed to upregulate TRAF6 expression (Figure 25A, B). In MM, TRAF6 mediates osteolytic bone lesions through the regulation of several downstream signaling pathways, including Akt, NFkB and p38MAPK (115), (116). So we next examined the activation of these downstream pathways of TRAF6 in BMM treated as described above. Western blot analysis demonstrated that the absence of CD166 on H929 or BMM decreased phospho AKT, phospho p38 and phospho IκBa levels (Figure 25A, C-E), indicating that loss of CD166 downregulates AKT, CD38MAPK and NFkB activation and most likely suppresses osteoclastogenesis.

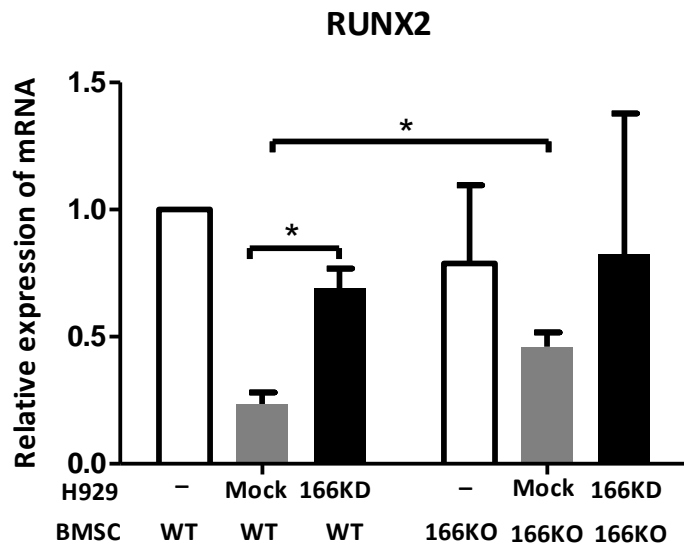
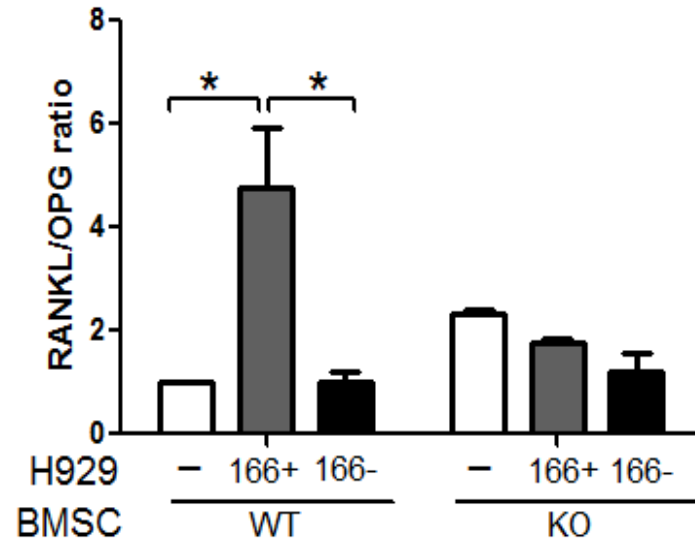


Figure 21. RUNX2 gene expression analysis on BMSC treated with H929 cells

RNA from BMSC cells cocultured with H929 cells (as indicated) for 48h before removal of the H929 cells and RNA isolation from the BMSC cells. Expression of RUNX2 was detected by quantitative PCR normalized to GAPDH and the “WT BMSC alone” sample. Two-way anova, * $p < 0.05$.

A



B

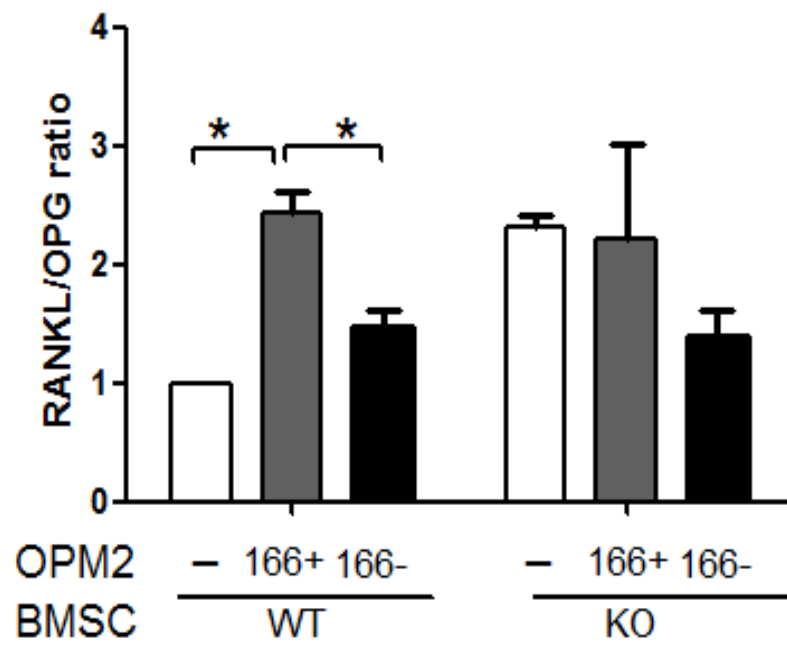


Figure 22. RANKL and OPG gene analysis on BMSC cocultured with H929 cells or OPM2 cells

(A) RNA from BMSC cells cocultured with H929 cells (as indicated) for 24h before removal of the H929 cells and RNA isolation from the BMSC cells.

Expression of RANKL and OPG was detected by quantitative PCR normalized to GAPDH and the “WT BMSC” sample. RANKL: OPG ratio was shown. (B) RNA from BMSC cells cocultured with H929 cells (as indicated) for 24h before removal of the H929 cells and RNA isolation from the BMSC cells. Expression of RANKL and OPG was detected by quantitative PCR normalized to GAPDH and the “WT BMSC” sample. RANKL: OPG ratio was shown. Two-way anova, * $p < 0.05$.

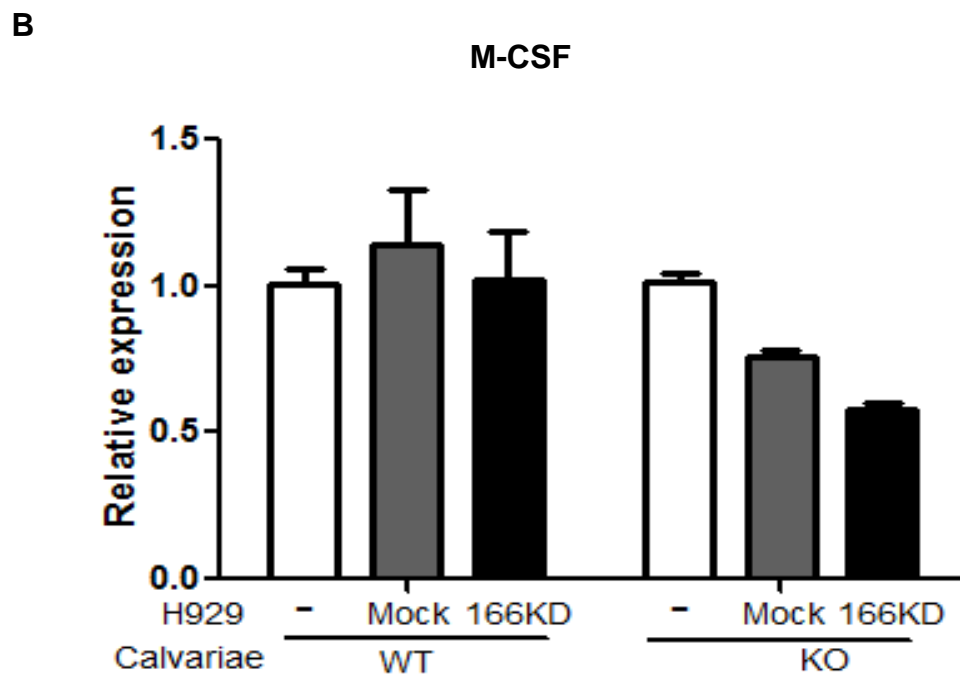
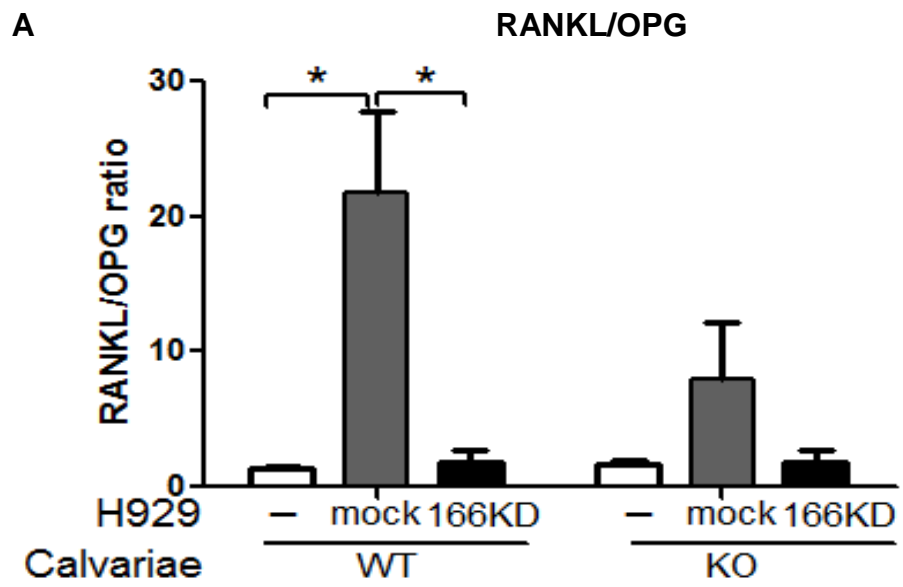


Figure 23. Osteoblastic gene analysis of calvariae cocultured with H929 cells

(A) RNA from calvarial cocultured with H929 cells (as indicated) for 7 days before removal of the H929 cells and RNA isolation from the calvarial. Expression of RANKL and OPG was detected by quantitative PCR relative to GAPDH and the “WT calvarial alone” sample. RANKL: OPG ratio was shown. (B) RNA from calvariae cocultured with H929 cells (as indicated) for 7 days were isolated after removal of the H929 cells. Expression of M-CSF was detected by quantitative PCR relative to GAPDH. Two-way anova, * $p < 0.05$.

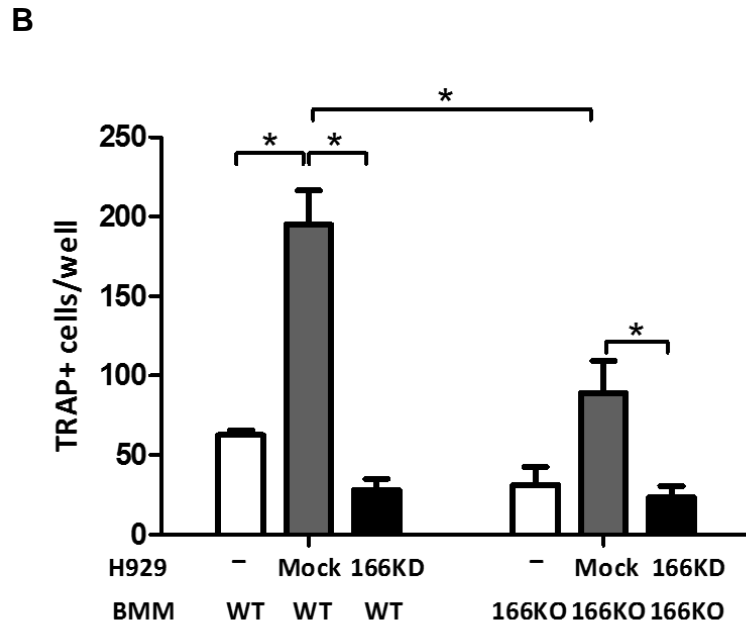
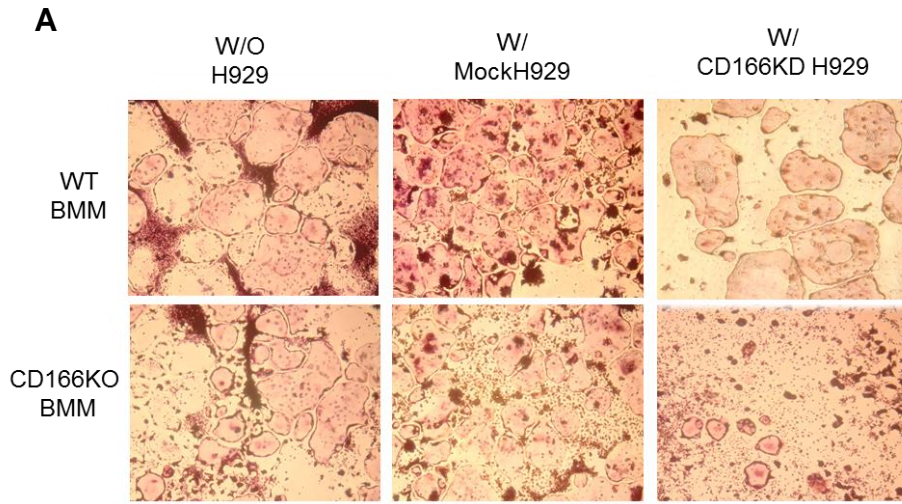


Figure 24. Osteoclast formation assay of BMM cells cocultured with mock or CD166KD H929 cells

(A) Non-adherent BM derived monocyte/macrophage from WT or CD166KO mice were cultured at a density of 65,000/cm² in α -MEM and supplemented with 10% FBS in the presence of recombinant mouse M-CSF (10 ng/ml) for 3 days to get adherent BMM. BMM were then cultured in α -MEM and supplemented with 10% FBS in the presence of recombinant mouse M-CSF (10 ng/ml) and RANKL (50ng/ml) for 7 days and mock H929 or CD166KD H929, followed by TRAP staining. (B)TRAP-positive MNCs from the whole culture were scored under a microscope. Data represent 3 separate experiments done in triplicates for each group are expressed as mean \pm SEM, Two-way anova, *p<0.05.

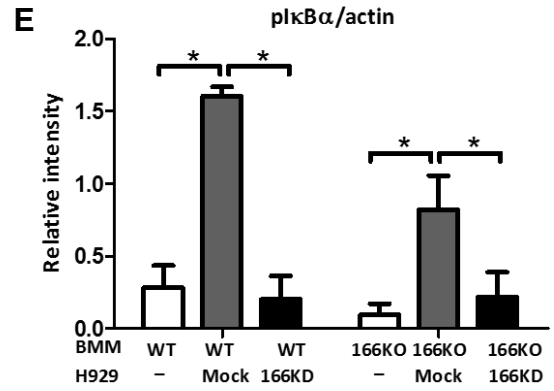
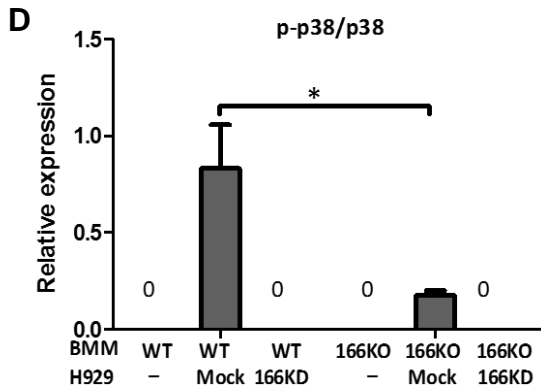
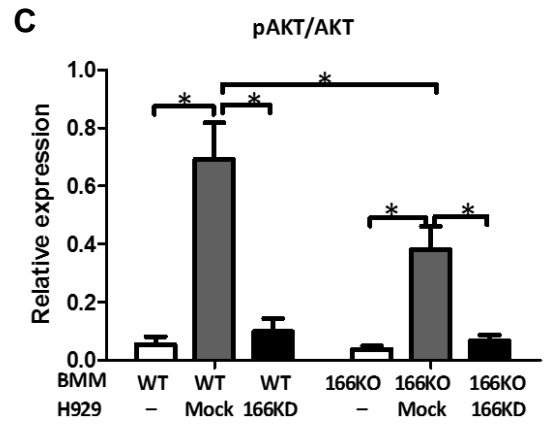
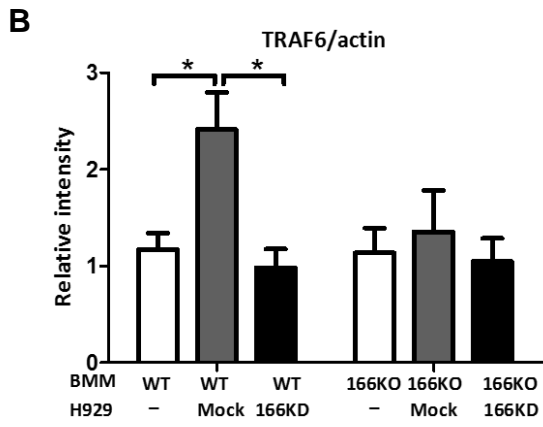
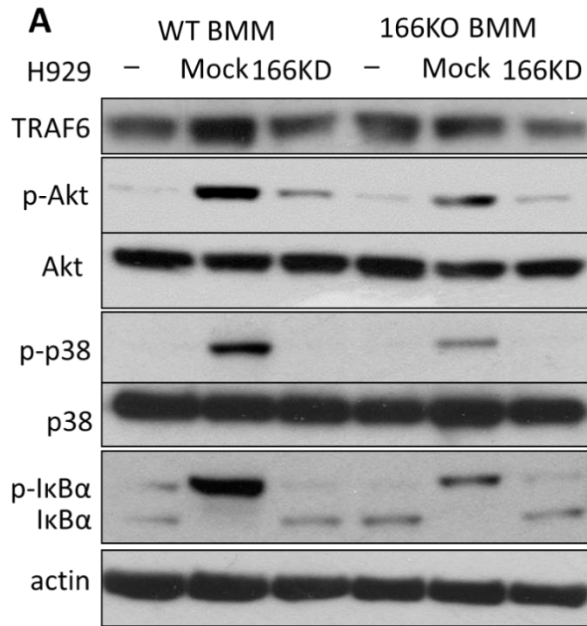


Figure 25. Absence of CD166 expression on MM cells downregulates key signaling pathways in osteoclastogenesis.

BMM were derived from bone marrow cells by culturing in the presence of M-CSF (10 ng/ml) for 3 days. (A-E) BMM were serum starved for 2h before exposure to mock H929 or CD166KD H929 for 30mins. H929 cells were washed off with cold PBS before the use of BMM in Western Blot analyses. BMM were then subjected to RIPA lysis and analyzed for the indicated proteins. Whole cell extracts were subjected to Western blot analysis with specific antibodies as indicated. Quantitative densitometry of the expression of the indicated proteins was normalized to actin protein expression. Data were collected from three separate observations and are expressed as mean \pm SEM. Two-way anova, *p<0.05.

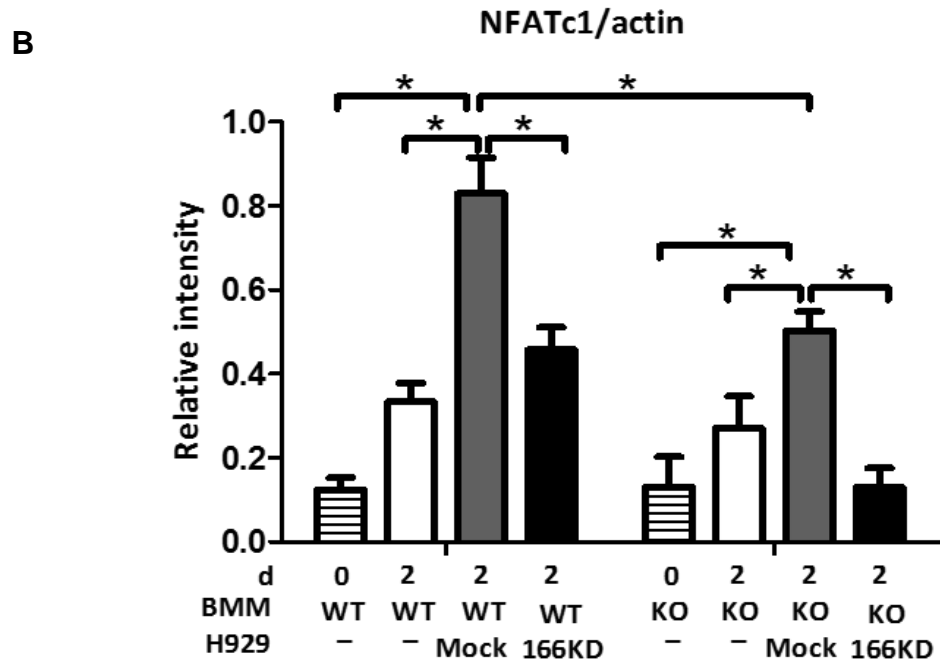
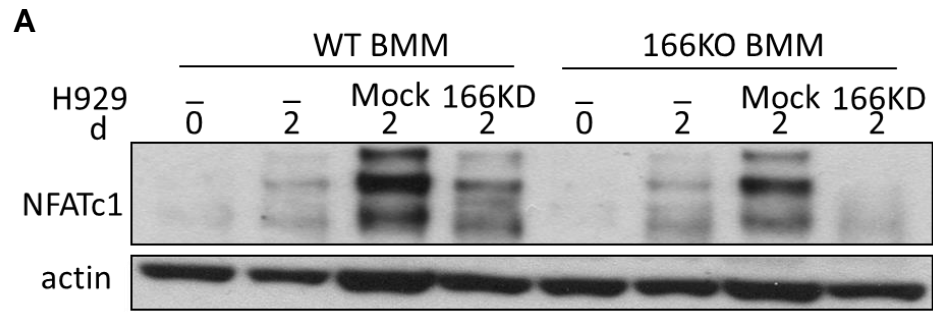


Figure 26. Absence of CD166 expression on MM cells NFATc1 in osteoclastogenesis

BMMs were derived from bone marrow cells by culturing in the presence of M-CSF (10 ng/ml) for 3 days. (A-B) BMM were cultured with mock H929 or CD166KD H929 in the presence of M-CSF (10 ng/ml) and RANKL (50ng/ml) for the indicated time. Whole cell extracts were subjected to Western blot analysis with specific Abs as indicated. Quantitative densitometry of the expression of the indicated proteins was normalized to actin protein expression. Data were collected from three separate observations and are expressed as mean± SEM. Two-way anova, *p<0.05.

Nuclear factor of activated T cells (NFAT)c1 is the key modulator in osteoclastogenesis (117). We further examined NFATc1 expression during osteoclastogenesis in our model. NFATc1 expression was strongly attenuated by the absence of CD166 expression on either H929 cells or BMMs (Figure 26A-B). Thus, CD166 regulate NFATc1 expression through regulating key signaling pathways during CD166 induced osteoclastogenesis in MM.

Discussion

Bone disease is a key complication in MM. Increased bone resorption in MM is due to osteoblast inhibition and osteoclast activation.

To determine the pathophysiologic effects of CD166 expression on MM bone disease, we used a novel EVOCA assay and found that CD166 can cause MM cells to induce bone destruction. Furthermore, the absence of CD166 on any cell type present in the EVOCA culture diminished this bone lytic disease. CD166 is a member of the immunoglobulin super family with 5 extracellular domains that can mediate homophilic (CD166-CD166) interactions (118). Therefore, the biochemical characteristic of CD166 and the results from the EVOCA assay suggest that homophilic interactions between MM cells and osteoblasts or other osteolineage cells expressing CD166 are critical for the progression of bone lytic disease. The fact that identical results were obtained when cells from two different MM cell lines and primary cells from 3 different patients were used in this assay, suggest that expression of CD166 or lack thereof is physiologically

relevant to MM. Bone remodeling is balanced by bone formation by osteoblasts and bone resorption by osteoclasts. However, this balance is broken or perturbed in the event of bone destruction (119,120). Therefore, it is possible that the change in bone remodeling observed in MM may result from CD166-mediated suppression of osteoblastogenesis or enhancement of osteoclastogenesis. Using in vitro assays, we demonstrated that expression of CD166 on MM cells promoted the repression of RUNX2, the key transcription factor in osteoblasts differentiation from BM-derived MSC (121). On the other hand, loss of CD166 on MM cells reduced the osteoclastogenic potential of BM-derived monocytes when these two cell types were co-cultured together suggesting that osteoclastogenesis was supported by CD166+ MM cells. In determining the molecular mechanisms underlying the CD166+ MM cell regulation of osteoclast formation, we observed that CD166 expression stimulated overexpression of RANKL while it failed to affect gene expression of OPG, an inhibitor of osteoclastogenesis, resulting in an increased RANKL: OPG ratio. We did not detect any significant difference in the gene expression of MSCF, suggesting the selective regulation of RANKL of CD166. Also this result is consistent with previous studies showing that increased RANKL: OPG ratio is the most important factor affecting osteoclastogenesis in MM (122). These observations implicate CD166 in the regulation of osteoclastogenesis through upregulation of RANKL and possibly downregulation or inhibition of OPG.

To further investigate how these effects are mediated by CD166, we examined the possible signaling pathways and revealed a possible novel positive regulatory pathway involving CD166-TRAF6 mediated osteoclast formation. Previous investigations demonstrated that TRAF6 is regulated by RANKL-RANK signaling pathway in osteoclastogenesis (49,123). Our studies documented an upregulation of TRAF6 in osteoclast precursors when these cells were stimulated by CD166+ MM cells. However, since we did not use RANKL for the stimulation, our study, for the first time, indicates that CD166 may regulate TRAF6 directly in osteoclastogenesis, suggesting that inhibition of CD166 may represent an effective way to control bone lytic disease in MM. Furthermore, we showed that the downstream signals of TRAF6, AKT, p38 and NFkB are downregulated by the absence of CD166 on MM cells. NFATc1, the important transcription factor in osteoclastogenesis, was also shown to be downregulated in the absence of CD166 from either MM cells or osteoclast precursors. However, further studies are needed to investigate the detailed mechanisms by which CD166 regulates RANKL and TRAF6 signaling pathways.

In conclusion, our data implicate CD166 in the progression of MM in vivo and suggest that this molecule is intimately involved in the pathogenesis of MM. That CD166 is a functional molecule that impacts HSC function and the competence of the normal hematopoietic niche, has been recently documented by our laboratory (78). Therefore, the question arises whether CD166 is expressed on MM initiating cells and whether this marker identifies a group of MM stem cells.

Given the involvement of CD166 in the pathophysiology of MM, CD166 could be a potential target for inhibiting the MM-induced osteolytic disease as well as tumor progression.

Chapter 4. Future Directions

The work presented here identified a critical role of CD166 in MM disease progression. CD166 is important for MM cells homing to the BM, enhancing disease progression and bone osteolytic diseases. Based on our findings, several possible future avenues should take and they are described in the following:

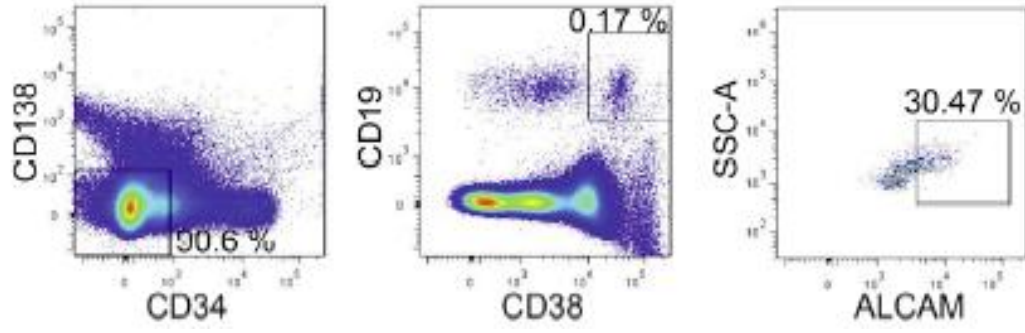
CD166 identifies MM stem cells

Despite therapeutic advances, MM remains incurable due to relapse and therapy-refractory disease. Persistence of drug-refractory MMSC provides a possible explanation for this clinical outcome. Targeting these cells is therefore appealing in MM therapy. Previously, our laboratory has demonstrated that CD166 is a key functional molecule on both human and murine HSC and HSC niche cells and that CD166+ fractions of murine and human repopulating HSC sustain robust long-term engraftment (78). Interestingly, MSC and osteoblasts, two critical components of the hematopoietic niche, also express CD166 (124). MM is a plasma cell malignancy in the BM. As a niche-dependent malignancy, and the cross-talk between MM cells and their BM niche is important for MM progression. Our current observations demonstrate that the interactions between MM cells and BM niche cells through CD166 is critical for MM disease progression and MM associated bone diseases. CD166+ MM cells home preferentially to the BM of NSG mice and cause more severe osteolytic lesions in

vivo. CD166 has been used to identify cancer stem cells in several other cancers, such as colorectal cancer (71), non-small cell lung cancer (81). Thus it is warranted and feasible to investigate whether CD166 is a possible marker for MMSC.

Matsui and colleagues identified a composite phenotype of MMSC as CD45+CD38+CD19+CD27+CD34-CD138- (59,60,125). They showed that CD34+CD19+CD138- but not their CD138+ counterpart MM cells were able to recapitulate MM in NOD-SCID mice. In our preliminary studies, when we used “Matsui” parameters to examine a newly diagnosed MM patient sample for the expression of CD166 on putative MMSC, about 30% of CD45+CD34-CD138-CD38+CD19+ cells were also CD166+ (Figure 27A), demonstrating that CD166 may identify a subset of MMSC. In addition, when we analyzed the MM cell line H929 (Figure 26B), we also found a similar expression level of CD166. These results indicate that both primary MM cells and the H929 MM cell line share a CD166+ population of putative MMSC. Future studies should investigate whether or not limiting number of CD166+ cells from primary patients’ samples or MM cell lines can initiate MM in mice models.

A



B

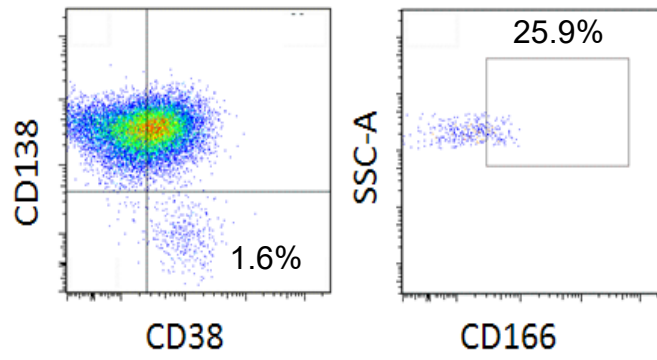


Figure 27. Primary MM cells and H929 share the same group of phenotypically defined putative MMSC expressing CD166

(A). BM cells from a MM patient were stained with “Matsui” markers and analyzed for CD166 expression on CD45+ CD38+CD19+CD27+CD34-CD138- cells. (B). CD166 expression on CD38+CD138- H929 cells.

Blocking CD166 with CD166 neutralizing antibody to abrogate disease progression

Antibody-based treatment in cancer therapy has been previously pursued in the last 2 or 3 decades with relative success (126-128). Monoclonal antibodies have great potential in the diagnosis and treatment of diseases (129). The mechanisms of action of the antibody therapy include direct tumor cell killing, immune-mediated tumor cell killing and vascular and stromal cell ablation (130). Although we did not observe any difference of the growth kinetics between mock H929 and CD166KD H929 cells (Figure 9), using anti-CD166 antibody to treat the H929 and 8226 MM cells every day for 5 days indicate that anti-CD166 antibody significantly inhibit the MM cell growth in vitro (Figure 28).

Recently, a CD166 neutralizing antibody fragment (single chain variable fragment) scFv173 has been shown to reduce cancer cell invasion and tumor growth in a breast cancer model (131). Since our findings demonstrated that CD166 is highly expressed on MM cells, it would be critical to know whether or not scFv173 can inhibit MM cell homing to the BM and further delay disease progression of MM.

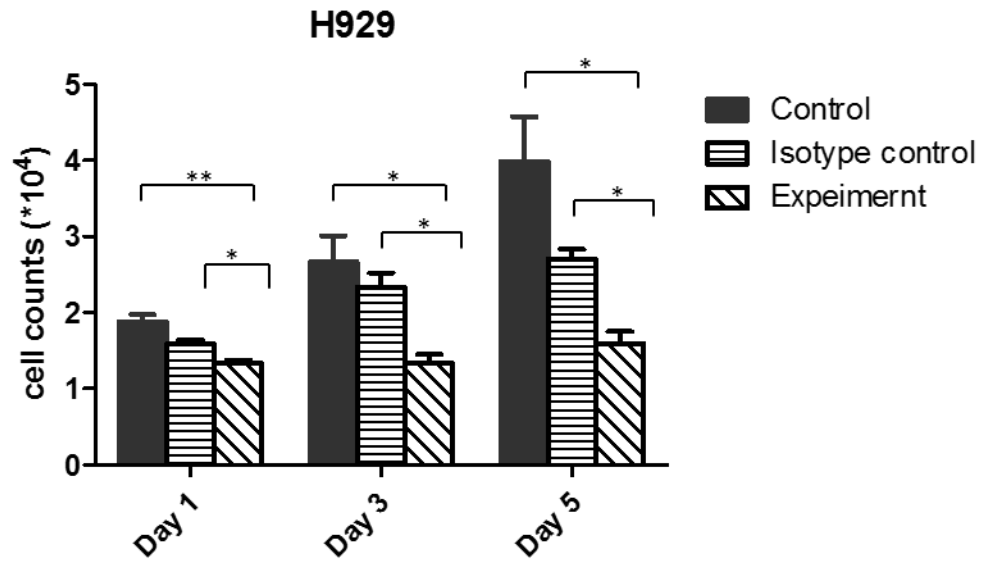
Determine with more details and particularly in the human system the role of CD166 in bone remodeling in MM

Bone remodeling in MM patients is broken to favor osteoclastogenesis while inhibiting osteoblastogenesis. Impaired osteoblasts development and bone formation contribute significantly to the osteolytic bone lesions associated with MM (132). In the present study, we have provided clear evidence that the expression of CD166 on MM cells downregulates RUNX2 gene expression on osteoblast precursors, indicating that MM cells may inhibit osteoblastogenesis of stromal cells in MM through the expression of CD166. However, the exact mechanisms behind this are not clear. Work by other groups indicate that cell-to-cell contact between stromal cells and MM cell are important for osteoblast activity inhibition (46,133). Further studies should explore whether the direct interactions between MM cells and osteoblast precursors through CD166 are critical for the osteoblast inhibition and the downstream signaling pathways through which the expression of CD166 on MM inhibits osteoblastogenesis and osteoblast functions.

Our result in the osteoclastogenesis assay (Figure 24) that the presence of CD166 on BMM cells contributes to the osteoclastogenesis in MM is striking. We also demonstrate that CD166 mediates TRAF6 and its downstream signaling pathways in osteoclastogenesis in MM. However, all of our current results are obtained with the murine system. Further studies should focus on setting up

experiments with human cells to examine the effects of MM cells on osteoclast activity.

A



B

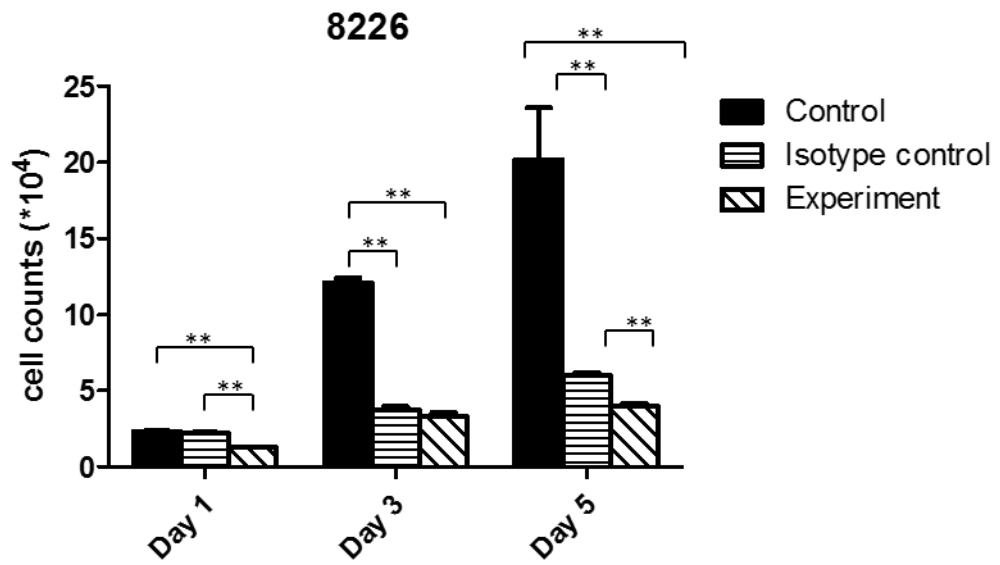


Figure 28. Anti-CD166 antibody inhibits MM cell growth

(A-B) H929 (A) or 8226 (B) were plated at 1.3×10^4 /well in 48 well-plate. Anti-CD166 antibody or isotype control were added to the well at 10ul/well every day for 5 days. Cell growth was quantified by counting the cell number with hemocytometer on days 1, 3 and 5. Two-way anova, * $p < 0.05$.

Reference

1. Bain G, Maandag EC, Izon DJ, Amsen D, Kruisbeek AM, Weintraub BC, et al. E2A proteins are required for proper B cell development and initiation of immunoglobulin gene rearrangements. *Cell* 1994;79(5):885-92.
2. Kim MS, Lapkouski M, Yang W, Gellert M. Crystal structure of the V(D)J recombinase RAG1-RAG2. *Nature* 2015;518(7540):507-11.
3. Vuyyuru R, Shen S, Manser T. Testing the role of the FcγRIIB immunoreceptor tyrosine-based inhibitory motif in regulation of the B cell immune response. *Immunity, inflammation and disease* 2015;3(3):247-64.
4. van Zelm MC, Szczepanski T, van der Burg M, van Dongen JJ. Replication history of B lymphocytes reveals homeostatic proliferation and extensive antigen-induced B cell expansion. *The Journal of experimental medicine* 2007;204(3):645-55.
5. Rollig C, Knop S, Bornhauser M. Multiple myeloma. *Lancet* 2015;385(9983):2197-208.
6. van de Donk NW, Palumbo A, Johnsen HE, Engelhardt M, Gay F, Gregersen H, et al. The clinical relevance and management of monoclonal gammopathy of undetermined significance and related disorders: recommendations from the European Myeloma Network. *Haematologica* 2014;99(6):984-96.

7. Boursi B, Weiss BM, Haynes K, Mamtani R, Yang YX. Reappraisal of risk factors for Monoclonal Gammopathy of Undetermined Significance. *American journal of hematology* 2016.
8. Anderson KC, Shaughnessy JD, Jr., Barlogie B, Harousseau JL, Roodman GD. Multiple myeloma. *Hematology / the Education Program of the American Society of Hematology American Society of Hematology Education Program* 2002:214-40.
9. Gonzalez D, van der Burg M, Garcia-Sanz R, Fenton JA, Langerak AW, Gonzalez M, et al. Immunoglobulin gene rearrangements and the pathogenesis of multiple myeloma. *Blood* 2007;110(9):3112-21.
10. Harada H, Kawano MM, Huang N, Harada Y, Iwato K, Tanabe O, et al. Phenotypic difference of normal plasma cells from mature myeloma cells. *Blood* 1993;81(10):2658-63.
11. Weisberger J, Wu CD, Liu Z, Wong JY, Melamed MR, Darzynkiewicz Z, et al. Differential diagnosis of malignant lymphomas and related disorders by specific pattern of expression of immunophenotypic markers revealed by multiparameter flow cytometry (Review). *International journal of oncology* 2000;17(6):1165-77.
12. Mali M, Jaakkola P, Arvilommi AM, Jalkanen M. Sequence of human syndecan indicates a novel gene family of integral membrane proteoglycans. *The Journal of biological chemistry* 1990;265(12):6884-9.

13. Elenius K, Salmivirta M, Inki P, Mali M, Jalkanen M. Binding of human syndecan to extracellular matrix proteins. *The Journal of biological chemistry* 1990;265(29):17837-43.
14. O'Connell FP, Pinkus JL, Pinkus GS. CD138 (syndecan-1), a plasma cell marker immunohistochemical profile in hematopoietic and nonhematopoietic neoplasms. *American journal of clinical pathology* 2004;121(2):254-63.
15. Lin P, Owens R, Tricot G, Wilson CS. Flow cytometric immunophenotypic analysis of 306 cases of multiple myeloma. *American journal of clinical pathology* 2004;121(4):482-8.
16. Kumar S, Kimlinger T, Morice W. Immunophenotyping in multiple myeloma and related plasma cell disorders. *Best practice & research Clinical haematology* 2010;23(3):433-51.
17. Frigyesi I, Adolfsson J, Ali M, Christophersen MK, Johnsson E, Turesson I, et al. Robust isolation of malignant plasma cells in multiple myeloma. *Blood* 2014;123(9):1336-40.
18. Damiano JS, Cress AE, Hazlehurst LA, Shtil AA, Dalton WS. Cell adhesion mediated drug resistance (CAM-DR): role of integrins and resistance to apoptosis in human myeloma cell lines. *Blood* 1999;93(5):1658-67.
19. Hazlehurst LA, Damiano JS, Buyuksal I, Pledger WJ, Dalton WS. Adhesion to fibronectin via beta1 integrins regulates p27kip1 levels and

- contributes to cell adhesion mediated drug resistance (CAM-DR).
Oncogene 2000;19(38):4319-27.
20. Pagnucco G, Cardinale G, Gervasi F. Targeting multiple myeloma cells and their bone marrow microenvironment. *Annals of the New York Academy of Sciences* 2004;1028:390-9.
 21. Givant-Horwitz V, Davidson B, Reich R. Laminin-induced signaling in tumor cells. *Cancer letters* 2005;223(1):1-10.
 22. Zdzisinska B, Walter-Croneck A, Kandefer-Szerszen M. Matrix metalloproteinases-1 and -2, and tissue inhibitor of metalloproteinase-2 production is abnormal in bone marrow stromal cells of multiple myeloma patients. *Leukemia research* 2008;32(11):1763-9.
 23. Fei M, Hang Q, Hou S, He S, Ruan C. Adhesion to fibronectin induces p27(Kip1) nuclear accumulation through down-regulation of Jab1 and contributes to cell adhesion-mediated drug resistance (CAM-DR) in RPMI 8,226 cells. *Molecular and cellular biochemistry* 2014;386(1-2):177-87.
 24. Fei M, Hang Q, Hou S, Ruan C. Cell adhesion to fibronectin down-regulates the expression of Spy1 and contributes to drug resistance in multiple myeloma cells. *International journal of hematology* 2013;98(4):446-55.
 25. Giuliani N, Storti P, Bolzoni M, Palma BD, Bonomini S. Angiogenesis and multiple myeloma. *Cancer microenvironment : official journal of the International Cancer Microenvironment Society* 2011;4(3):325-37.

26. Rosean TR, Tompkins VS, Tricot G, Holman CJ, Olivier AK, Zhan F, et al. Preclinical validation of interleukin 6 as a therapeutic target in multiple myeloma. *Immunologic research* 2014;59(1-3):188-202.
27. Ferrara N. Role of vascular endothelial growth factor in regulation of physiological angiogenesis. *American journal of physiology Cell physiology* 2001;280(6):C1358-66.
28. Kumar S, Witzig TE, Timm M, Haug J, Wellik L, Fonseca R, et al. Expression of VEGF and its receptors by myeloma cells. *Leukemia : official journal of the Leukemia Society of America, Leukemia Research Fund, UK* 2003;17(10):2025-31.
29. Tjin EP, Derksen PW, Kataoka H, Spaargaren M, Pals ST. Multiple myeloma cells catalyze hepatocyte growth factor (HGF) activation by secreting the serine protease HGF-activator. *Blood* 2004;104(7):2172-5.
30. Ukaji T, Hashimoto M, Kai O. Conditioned medium from gerbil--mouse T cell heterohybridomas improved antibody secretion. *Experimental animals / Japanese Association for Laboratory Animal Science* 2015;64(2):199-205.
31. Trentin L, Miorin M, Facco M, Baesso I, Carraro S, Cabrelle A, et al. Multiple myeloma plasma cells show different chemokine receptor profiles at sites of disease activity. *British journal of haematology* 2007;138(5):594-602.
32. Vande Broek I, Leleu X, Schots R, Facon T, Vanderkerken K, Van Camp B, et al. Clinical significance of chemokine receptor (CCR1, CCR2 and

- CXCR4) expression in human myeloma cells: the association with disease activity and survival. *Haematologica* 2006;91(2):200-6.
33. Wada A, Ito A, Iitsuka H, Tsuneyama K, Miyazono T, Murakami J, et al. Role of chemokine CX3CL1 in progression of multiple myeloma via CX3CR1 in bone microenvironments. *Oncology reports* 2015;33(6):2935-9.
 34. Bao L, Lai Y, Liu Y, Qin Y, Zhao X, Lu X, et al. CXCR4 is a good survival prognostic indicator in multiple myeloma patients. *Leukemia research* 2013;37(9):1083-8.
 35. Azab AK, Runnels JM, Pitsillides C, Moreau AS, Azab F, Leleu X, et al. CXCR4 inhibitor AMD3100 disrupts the interaction of multiple myeloma cells with the bone marrow microenvironment and enhances their sensitivity to therapy. *Blood* 2009;113(18):4341-51.
 36. Kim J, Denu RA, Dollar BA, Escalante LE, Kuether JP, Callander NS, et al. Macrophages and mesenchymal stromal cells support survival and proliferation of multiple myeloma cells. *British journal of haematology* 2012.
 37. Zheng Y, Cai Z, Wang S, Zhang X, Qian J, Hong S, et al. Macrophages are an abundant component of myeloma microenvironment and protect myeloma cells from chemotherapy drug-induced apoptosis. *Blood* 2009;114(17):3625-8.
 38. Pellegrino A, Ria R, Di Pietro G, Cirulli T, Surico G, Pennisi A, et al. Bone marrow endothelial cells in multiple myeloma secrete CXC-chemokines

that mediate interactions with plasma cells. *British journal of haematology* 2005;129(2):248-56.

39. Ria R, Todoerti K, Berardi S, Coluccia AM, De Luisi A, Mattioli M, et al. Gene expression profiling of bone marrow endothelial cells in patients with multiple myeloma. *Clinical cancer research : an official journal of the American Association for Cancer Research* 2009;15(17):5369-78.
40. Costantini R, Manfredi MT, Iori A, Pacetti A. *Protostrongylus pulmonalis* from hares (*Lepus europaeus*) in Italy. *Parassitologia* 1990;32(3):353-7.
41. Otto F, Kanegane H, Mundlos S. Mutations in the RUNX2 gene in patients with cleidocranial dysplasia. *Human mutation* 2002;19(3):209-16.
42. Hecht J, Seitz V, Urban M, Wagner F, Robinson PN, Stiege A, et al. Detection of novel skeletogenesis target genes by comprehensive analysis of a Runx2(-/-) mouse model. *Gene expression patterns : GEP* 2007;7(1-2):102-12.
43. Vaes BL, Ducy P, Sijbers AM, Hendriks JM, van Someren EP, de Jong NG, et al. Microarray analysis on Runx2-deficient mouse embryos reveals novel Runx2 functions and target genes during intramembranous and endochondral bone formation. *Bone* 2006;39(4):724-38.
44. Jeon MJ, Kim JA, Kwon SH, Kim SW, Park KS, Park SW, et al. Activation of peroxisome proliferator-activated receptor-gamma inhibits the Runx2-mediated transcription of osteocalcin in osteoblasts. *The Journal of biological chemistry* 2003;278(26):23270-7.

45. Gersbach CA, Byers BA, Pavlath GK, Garcia AJ. Runx2/Cbfa1 stimulates transdifferentiation of primary skeletal myoblasts into a mineralizing osteoblastic phenotype. *Experimental cell research* 2004;300(2):406-17.
46. Giuliani N, Colla S, Morandi F, Lazzaretti M, Sala R, Bonomini S, et al. Myeloma cells block RUNX2/CBFA1 activity in human bone marrow osteoblast progenitors and inhibit osteoblast formation and differentiation. *Blood* 2005;106(7):2472-83.
47. Glantschnig H, Fisher JE, Wesolowski G, Rodan GA, Reszka AA. M-CSF, TNFalpha and RANK ligand promote osteoclast survival by signaling through mTOR/S6 kinase. *Cell death and differentiation* 2003;10(10):1165-77.
48. Lai FP, Cole-Sinclair M, Cheng WJ, Quinn JM, Gillespie MT, Sentry JW, et al. Myeloma cells can directly contribute to the pool of RANKL in bone bypassing the classic stromal and osteoblast pathway of osteoclast stimulation. *British journal of haematology* 2004;126(2):192-201.
49. Lamothe B, Webster WK, Gopinathan A, Besse A, Campos AD, Darnay BG. TRAF6 ubiquitin ligase is essential for RANKL signaling and osteoclast differentiation. *Biochemical and biophysical research communications* 2007;359(4):1044-9.
50. Lomaga MA, Yeh WC, Sarosi I, Duncan GS, Furlonger C, Ho A, et al. TRAF6 deficiency results in osteopetrosis and defective interleukin-1, CD40, and LPS signaling. *Genes & development* 1999;13(8):1015-24.

51. Naito A, Yoshida H, Nishioka E, Satoh M, Azuma S, Yamamoto T, et al. TRAF6-deficient mice display hypohidrotic ectodermal dysplasia. *Proceedings of the National Academy of Sciences of the United States of America* 2002;99(13):8766-71.
52. Chung JY, Park YC, Ye H, Wu H. All TRAFs are not created equal: common and distinct molecular mechanisms of TRAF-mediated signal transduction. *Journal of cell science* 2002;115(Pt 4):679-88.
53. Wu H, Arron JR. TRAF6, a molecular bridge spanning adaptive immunity, innate immunity and osteoimmunology. *BioEssays : news and reviews in molecular, cellular and developmental biology* 2003;25(11):1096-105.
54. Liu H, Tamashiro S, Baritaki S, Penichet M, Yu Y, Chen H, et al. TRAF6 activation in multiple myeloma: a potential therapeutic target. *Clinical lymphoma, myeloma & leukemia* 2012;12(3):155-63.
55. Wang X, Wang J, Liu H, Xu R, Ding R, Jiang S, et al. TRAF6 is required for BLyS-mediated NF-kappaB signaling in multiple myeloma cells. *Medical oncology* 2015;32(10):239.
56. Dick JE. Stem cell concepts renew cancer research. *Blood* 2008;112(13):4793-807.
57. Alison MR, Guppy NJ, Lim SM, Nicholson LJ. Finding cancer stem cells: are aldehyde dehydrogenases fit for purpose? *The Journal of pathology* 2010;222(4):335-44.

58. Moitra K, Lou H, Dean M. Multidrug efflux pumps and cancer stem cells: insights into multidrug resistance and therapeutic development. *Clinical pharmacology and therapeutics* 2011;89(4):491-502.
59. Matsui W, Huff CA, Wang Q, Malehorn MT, Barber J, Tanhehco Y, et al. Characterization of clonogenic multiple myeloma cells. *Blood* 2004;103(6):2332-6.
60. Matsui W, Wang Q, Barber JP, Brennan S, Smith BD, Borrello I, et al. Clonogenic multiple myeloma progenitors, stem cell properties, and drug resistance. *Cancer research* 2008;68(1):190-7.
61. Kuranda K, Berthon C, Dupont C, Wolowiec D, Leleu X, Polakowska R, et al. A subpopulation of malignant CD34+CD138+B7-H1+ plasma cells is present in multiple myeloma patients. *Experimental hematology* 2010;38(2):124-31.
62. Goodell MA, Brose K, Paradis G, Conner AS, Mulligan RC. Isolation and functional properties of murine hematopoietic stem cells that are replicating in vivo. *The Journal of experimental medicine* 1996;183(4):1797-806.
63. Ramos CA, Venezia TA, Camargo FA, Goodell MA. Techniques for the study of adult stem cells: be fruitful and multiply. *BioTechniques* 2003;34(3):572-8, 80-4, 86-91.
64. Yaccoby S, Barlogie B, Epstein J. Primary myeloma cells growing in SCID-hu mice: a model for studying the biology and treatment of myeloma and its manifestations. *Blood* 1998;92(8):2908-13.

65. Yaccoby S, Epstein J. The proliferative potential of myeloma plasma cells manifest in the SCID-hu host. *Blood* 1999;94(10):3576-82.
66. Bowen MA, Patel DD, Li X, Modrell B, Malacko AR, Wang WC, et al. Cloning, mapping, and characterization of activated leukocyte-cell adhesion molecule (ALCAM), a CD6 ligand. *The Journal of experimental medicine* 1995;181(6):2213-20.
67. van Kempen LC, Nelissen JM, Degen WG, Torensma R, Weidle UH, Bloemers HP, et al. Molecular basis for the homophilic activated leukocyte cell adhesion molecule (ALCAM)-ALCAM interaction. *The Journal of biological chemistry* 2001;276(28):25783-90.
68. Bowen MA, Aruffo AA, Bajorath J. Cell surface receptors and their ligands: in vitro analysis of CD6-CD166 interactions. *Proteins* 2000;40(3):420-8.
69. Chappell PE, Garner LI, Yan J, Metcalfe C, Hatherley D, Johnson S, et al. Structures of CD6 and Its Ligand CD166 Give Insight into Their Interaction. *Structure* 2015;23(8):1426-36.
70. Bowen MA, Bajorath J, D'Egidio M, Whitney GS, Palmer D, Kobarg J, et al. Characterization of mouse ALCAM (CD166): the CD6-binding domain is conserved in different homologs and mediates cross-species binding. *European journal of immunology* 1997;27(6):1469-78.
71. Levin TG, Powell AE, Davies PS, Silk AD, Dismuke AD, Anderson EC, et al. Characterization of the intestinal cancer stem cell marker CD166 in the human and mouse gastrointestinal tract. *Gastroenterology* 2010;139(6):2072-82 e5.

72. Cayrol R, Wosik K, Berard JL, Dodelet-Devillers A, Ifergan I, Kebir H, et al. Activated leukocyte cell adhesion molecule promotes leukocyte trafficking into the central nervous system. *Nature immunology* 2008;9(2):137-45.
73. Masedunskas A, King JA, Tan F, Cochran R, Stevens T, Sviridov D, et al. Activated leukocyte cell adhesion molecule is a component of the endothelial junction involved in transendothelial monocyte migration. *FEBS letters* 2006;580(11):2637-45.
74. Jezierska A, Matysiak W, Motyl T. ALCAM/CD166 protects breast cancer cells against apoptosis and autophagy. *Medical science monitor : international medical journal of experimental and clinical research* 2006;12(8):BR263-73.
75. Swart GW, Lunter PC, Kilsdonk JW, Kempen LC. Activated leukocyte cell adhesion molecule (ALCAM/CD166): signaling at the divide of melanoma cell clustering and cell migration? *Cancer metastasis reviews* 2005;24(2):223-36.
76. van Kempen LC, van den Oord JJ, van Muijen GN, Weidle UH, Bloemers HP, Swart GW. Activated leukocyte cell adhesion molecule/CD166, a marker of tumor progression in primary malignant melanoma of the skin. *The American journal of pathology* 2000;156(3):769-74.
77. Rajasekhar VK, Studer L, Gerald W, Socci ND, Scher HI. Tumour-initiating stem-like cells in human prostate cancer exhibit increased NF-kappaB signalling. *Nature communications* 2011;2:162.

78. Chitteti BR, Kobayashi M, Cheng Y, Zhang H, Poteat BA, Broxmeyer HE, et al. CD166 regulates human and murine hematopoietic stem cells and the hematopoietic niche. *Blood* 2014;124(4):519-29.
79. Bruder SP, Ricalton NS, Boynton RE, Connolly TJ, Jaiswal N, Zaia J, et al. Mesenchymal stem cell surface antigen SB-10 corresponds to activated leukocyte cell adhesion molecule and is involved in osteogenic differentiation. *Journal of bone and mineral research : the official journal of the American Society for Bone and Mineral Research* 1998;13(4):655-63.
80. Wang J, Gu Z, Ni P, Qiao Y, Chen C, Liu X, et al. NF-kappaB P50/P65 hetero-dimer mediates differential regulation of CD166/ALCAM expression via interaction with microRNA-9 after serum deprivation, providing evidence for a novel negative auto-regulatory loop. *Nucleic acids research* 2011;39(15):6440-55.
81. Gilsanz A, Sanchez-Martin L, Gutierrez-Lopez MD, Ovalle S, Machado-Pineda Y, Reyes R, et al. ALCAM/CD166 adhesive function is regulated by the tetraspanin CD9. *Cellular and molecular life sciences : CMLS* 2013;70(3):475-93.
82. Tachezy M, Effenberger K, Zander H, Minner S, Gebauer F, Vashist YK, et al. ALCAM (CD166) expression and serum levels are markers for poor survival of esophageal cancer patients. *International journal of cancer Journal international du cancer* 2012;131(2):396-405.

83. Witzig TE, Kimlinger TK, Ahmann GJ, Katzmann JA, Greipp PR. Detection of myeloma cells in the peripheral blood by flow cytometry. *Cytometry* 1996;26(2):113-20.
84. Alsayed Y, Ngo H, Runnels J, Leleu X, Singha UK, Pitsillides CM, et al. Mechanisms of regulation of CXCR4/SDF-1 (CXCL12)-dependent migration and homing in multiple myeloma. *Blood* 2007;109(7):2708-17.
85. Glavey SV, Manier S, Natoni A, Sacco A, Moschetta M, Reagan MR, et al. The sialyltransferase ST3GAL6 influences homing and survival in multiple myeloma. *Blood* 2014;124(11):1765-76.
86. Chitteti BR, Cheng YH, Kacena MA, Srour EF. Hierarchical organization of osteoblasts reveals the significant role of CD166 in hematopoietic stem cell maintenance and function. *Bone* 2013;54(1):58-67.
87. Yusuf RZ, Scadden DT. Homing of hematopoietic cells to the bone marrow. *Journal of visualized experiments : JoVE* 2009(25).
88. Jetmore A, Plett PA, Tong X, Wolber FM, Breese R, Abonour R, et al. Homing efficiency, cell cycle kinetics, and survival of quiescent and cycling human CD34(+) cells transplanted into conditioned NOD/SCID recipients. *Blood* 2002;99(5):1585-93.
89. Hall KM, Horvath TL, Abonour R, Cornetta K, Srour EF. Decreased homing of retrovirally transduced human bone marrow CD34+ cells in the NOD/SCID mouse model. *Experimental hematology* 2006;34(4):433-42.

90. Kawano Y, Moschetta M, Manier S, Glavey S, Gorgun GT, Roccaro AM, et al. Targeting the bone marrow microenvironment in multiple myeloma. *Immunological reviews* 2015;263(1):160-72.
91. Mitsiades CS, McMillin DW, Klippel S, Hideshima T, Chauhan D, Richardson PG, et al. The role of the bone marrow microenvironment in the pathophysiology of myeloma and its significance in the development of more effective therapies. *Hematology/oncology clinics of North America* 2007;21(6):1007-34, vii-viii.
92. Roodman GD. Pathogenesis of myeloma bone disease. *Blood cells, molecules & diseases* 2004;32(2):290-2.
93. Chitteti BR, Bethel M, Kacena MA, Srour EF. CD166 and regulation of hematopoiesis. *Current opinion in hematology* 2013;20(4):273-80.
94. Weidle UH, Eggle D, Klostermann S, Swart GW. ALCAM/CD166: cancer-related issues. *Cancer genomics & proteomics* 2010;7(5):231-43.
95. Slovak ML. Multiple myeloma: current perspectives. *Clinics in laboratory medicine* 2011;31(4):699-724, x.
96. Podar K, Chauhan D, Anderson KC. Bone marrow microenvironment and the identification of new targets for myeloma therapy. *Leukemia : official journal of the Leukemia Society of America, Leukemia Research Fund, UK* 2009;23(1):10-24.
97. Oyajobi BO, Franchin G, Williams PJ, Pulkrabek D, Gupta A, Munoz S, et al. Dual effects of macrophage inflammatory protein-1alpha on osteolysis

- and tumor burden in the murine 5TGM1 model of myeloma bone disease. *Blood* 2003;102(1):311-9.
98. Sati HI, Greaves M, Apperley JF, Russell RG, Croucher PI. Expression of interleukin-1beta and tumour necrosis factor-alpha in plasma cells from patients with multiple myeloma. *British journal of haematology* 1999;104(2):350-7.
99. Mitsiades CS, Mitsiades NS, Munshi NC, Richardson PG, Anderson KC. The role of the bone microenvironment in the pathophysiology and therapeutic management of multiple myeloma: interplay of growth factors, their receptors and stromal interactions. *European journal of cancer* 2006;42(11):1564-73.
100. Zannettino AC, Farrugia AN, Kortesidis A, Manavis J, To LB, Martin SK, et al. Elevated serum levels of stromal-derived factor-1alpha are associated with increased osteoclast activity and osteolytic bone disease in multiple myeloma patients. *Cancer research* 2005;65(5):1700-9.
101. Lee JW, Chung HY, Ehrlich LA, Jelinek DF, Callander NS, Roodman GD, et al. IL-3 expression by myeloma cells increases both osteoclast formation and growth of myeloma cells. *Blood* 2004;103(6):2308-15.
102. Hsu H, Lacey DL, Dunstan CR, Solovyev I, Colombero A, Timms E, et al. Tumor necrosis factor receptor family member RANK mediates osteoclast differentiation and activation induced by osteoprotegerin ligand. *Proceedings of the National Academy of Sciences of the United States of America* 1999;96(7):3540-5.

103. Dougall WC, Glaccum M, Charrier K, Rohrbach K, Brasel K, De Smedt T, et al. RANK is essential for osteoclast and lymph node development. *Genes & development* 1999;13(18):2412-24.
104. Lacey DL, Timms E, Tan HL, Kelley MJ, Dunstan CR, Burgess T, et al. Osteoprotegerin ligand is a cytokine that regulates osteoclast differentiation and activation. *Cell* 1998;93(2):165-76.
105. Hofbauer LC, Khosla S, Dunstan CR, Lacey DL, Boyle WJ, Riggs BL. The roles of osteoprotegerin and osteoprotegerin ligand in the paracrine regulation of bone resorption. *Journal of bone and mineral research : the official journal of the American Society for Bone and Mineral Research* 2000;15(1):2-12.
106. Komori T, Yagi H, Nomura S, Yamaguchi A, Sasaki K, Deguchi K, et al. Targeted disruption of Cbfa1 results in a complete lack of bone formation owing to maturational arrest of osteoblasts. *Cell* 1997;89(5):755-64.
107. Weitzmann MN, Roggia C, Toraldo G, Weitzmann L, Pacifici R. Increased production of IL-7 uncouples bone formation from bone resorption during estrogen deficiency. *The Journal of clinical investigation* 2002;110(11):1643-50.
108. Qiang YW, Hu B, Chen Y, Zhong Y, Shi B, Barlogie B, et al. Bortezomib induces osteoblast differentiation via Wnt-independent activation of beta-catenin/TCF signaling. *Blood* 2009;113(18):4319-30.
109. Mohammad KS, Chirgwin JM, Guise TA. Assessing new bone formation in neonatal calvarial organ cultures. *Methods Mol Biol* 2008;455:37-50.

110. Wei S, Wang MW, Teitelbaum SL, Ross FP. Interleukin-4 reversibly inhibits osteoclastogenesis via inhibition of NF-kappa B and mitogen-activated protein kinase signaling. *The Journal of biological chemistry* 2002;277(8):6622-30.
111. Soleimani M, Nadri S. A protocol for isolation and culture of mesenchymal stem cells from mouse bone marrow. *Nature protocols* 2009;4(1):102-6.
112. Ross FP. M-CSF, c-Fms, and signaling in osteoclasts and their precursors. *Annals of the New York Academy of Sciences* 2006;1068:110-6.
113. Kim K, Kim JH, Lee J, Jin HM, Kook H, Kim KK, et al. MafB negatively regulates RANKL-mediated osteoclast differentiation. *Blood* 2007;109(8):3253-9.
114. Lamothe B, Campos AD, Webster WK, Gopinathan A, Hur L, Darnay BG. The RING domain and first zinc finger of TRAF6 coordinate signaling by interleukin-1, lipopolysaccharide, and RANKL. *The Journal of biological chemistry* 2008;283(36):24871-80.
115. Adamopoulos IE, Mellins ED. Alternative pathways of osteoclastogenesis in inflammatory arthritis. *Nature reviews Rheumatology* 2015;11(3):189-94.
116. Moon JB, Kim JH, Kim K, Youn BU, Ko A, Lee SY, et al. Akt induces osteoclast differentiation through regulating the GSK3beta/NFATc1 signaling cascade. *J Immunol* 2012;188(1):163-9.

117. Takayanagi H. The role of NFAT in osteoclast formation. *Annals of the New York Academy of Sciences* 2007;1116:227-37.
118. Swart GW. Activated leukocyte cell adhesion molecule (CD166/ALCAM): developmental and mechanistic aspects of cell clustering and cell migration. *European journal of cell biology* 2002;81(6):313-21.
119. Roodman GD. Mechanisms of bone metastasis. *The New England journal of medicine* 2004;350(16):1655-64.
120. Reagan MR, Liaw L, Rosen CJ, Ghobrial IM. Dynamic interplay between bone and multiple myeloma: emerging roles of the osteoblast. *Bone* 2015;75:161-9.
121. Marie PJ. Transcription factors controlling osteoblastogenesis. *Archives of biochemistry and biophysics* 2008;473(2):98-105.
122. Zdzisinska B, Kandefer-Szerszen M. [The role of RANK/RANKL and OPG in multiple myeloma]. *Postepy higieny i medycyny doswiadczalnej* 2006;60:471-82.
123. Takayanagi H, Ogasawara K, Hida S, Chiba T, Murata S, Sato K, et al. T-cell-mediated regulation of osteoclastogenesis by signalling cross-talk between RANKL and IFN-gamma. *Nature* 2000;408(6812):600-5.
124. Halfon S, Abramov N, Grinblat B, Ginis I. Markers distinguishing mesenchymal stem cells from fibroblasts are downregulated with passaging. *Stem cells and development* 2011;20(1):53-66.
125. Peacock CD, Wang Q, Gesell GS, Corcoran-Schwartz IM, Jones E, Kim J, et al. Hedgehog signaling maintains a tumor stem cell compartment in

- multiple myeloma. Proceedings of the National Academy of Sciences of the United States of America 2007;104(10):4048-53.
126. Scott AM, Lee FT, Tebbutt N, Herbertson R, Gill SS, Liu Z, et al. A phase I clinical trial with monoclonal antibody ch806 targeting transitional state and mutant epidermal growth factor receptors. Proceedings of the National Academy of Sciences of the United States of America 2007;104(10):4071-6.
127. Hodi FS, O'Day SJ, McDermott DF, Weber RW, Sosman JA, Haanen JB, et al. Improved survival with ipilimumab in patients with metastatic melanoma. The New England journal of medicine 2010;363(8):711-23.
128. Caron PC, Jurcic JG, Scott AM, Finn RD, Divgi CR, Graham MC, et al. A phase 1B trial of humanized monoclonal antibody M195 (anti-CD33) in myeloid leukemia: specific targeting without immunogenicity. Blood 1994;83(7):1760-8.
129. Nelson AL, Reichert JM. Development trends for therapeutic antibody fragments. Nature biotechnology 2009;27(4):331-7.
130. Scott AM, Wolchok JD, Old LJ. Antibody therapy of cancer. Nature reviews Cancer 2012;12(4):278-87.
131. Wiiger MT, Gehrken HB, Fodstad O, Maelandsmo GM, Andersson Y. A novel human recombinant single-chain antibody targeting CD166/ALCAM inhibits cancer cell invasion in vitro and in vivo tumour growth. Cancer immunology, immunotherapy : CII 2010;59(11):1665-74.

132. Giuliani N, Rizzoli V, Roodman GD. Multiple myeloma bone disease: Pathophysiology of osteoblast inhibition. *Blood* 2006;108(13):3992-6.
133. Mori Y, Shimizu N, Dallas M, Niewolna M, Story B, Williams PJ, et al. Anti-alpha4 integrin antibody suppresses the development of multiple myeloma and associated osteoclastic osteolysis. *Blood* 2004;104(7):2149-54.

Curriculum Vitae

Linlin Xu

Education

Indiana University, Indianapolis, Indiana, USA

Ph.D. Microbiology and Immunology Aug 2010 – June 2016

Peking Union Medical College, Tianjin, China

M.S. Biomedical Science Sep 2007 – July 2010

Shandong University, Weihai, Shandong, China

B.S. Biological Science Sep 2003 – Sep 2007

Research Experience

Dr. Edward F. Srouf laboratory, Indiana University School of Medicine

Graduate student, Department of Microbiology and Immunology

May 2011- June 2016

Project 1: Identifying the role of CD166 in multiple myeloma disease progression and osteolytic bone diseases.

Project 2: Studying the role of novel macrophage subset - OsteoMacs in sustaining the competence of the hematopoietic niche and the hematopoietic stem cell function.

Dr. Guoguang Zheng laboratory, Peking Union Medical College

Research Assistant, Institute of Hematology and Blood Disease Hospital

Sep 2007 – July 2010

Project: Examined the effect of membrane form of macrophage stimulating factor on the polarization of macrophages

Teaching Experience

Teaching Assistant

Microbiology and Immunology undergraduate course Aug 2012 – Dec 2012

Publications

Xu LL, Mohammad KS, Wu H, Crean C, Machal C , Poteat B, Cheng YH, Cardoso AA, Kacena MA, Hanenberg H, Abonour R, Suvannasankha A, Srour EF. CD166 Mediates Multiple Myeloma Cells Homing to the Bone Marrow Microenvironment and Promotes Myeloma Disease Progression (Cancer Research)

Xu LL, Himes E, Wu H, Cheng YH, Mohamand S, Davis K, Kacena MA, Srour EF. A novel CD45+ population within calvariae regulates hematopoietic stem cell functions (Stem cell Reports, Under Review)

Alvarez MB, **Xu LL**, Himes E, Chitteti BR, Childress P, Cheng YH, Srour EF, Kacena MA Regulation of the Hematopoietic Niche by Megakaryocyte-Osteoblast Interactions (in preparation)

Wu H, **Xu LL**, Teuscher P, Liu H, Kaplan MK, Dent AL. An Inhibitory Role for the Transcription Factor Stat3 in Controlling IL-4 and Bcl6 Expression in Follicular Helper T Cells. *The Journal of Immunology*, 2015, 195: 2080–2089.

Wu H, Chen YX, Liu H, **Xu LL**, Teuscher P, Wang SX, Lu S, Dent AL. Follicular Regulatory T cells

Repress Cytokine Production by Follicular Helper T cells and Optimize IgG Responses in mice. *Eur J Immuno* (Accepted)

Ma CH, Chong JH, Guo Y, Zeng HM, Liu SY, **Xu LL**, et al, Abnormal expression of ADAR1 isoforms in Chinese pediatric acute leukemias. *Biochem Biophys Res Commun*, 2011 Mar 11;406(2):245-51

Xu LL, Zheng GG, Ma CH, et al, Role of mM-CSF on the functional differentiation of macrophage. *Journal of Leukemia&Lymphoma*, 2010 Vol. 19 (7): 388-390

Meeting Presentations

Xu LL, Machal C, Wu H, et al, CD166 Facilitates Multiple Myeloma Cells Homing to the Bone Marrow Microenvironment and Promote Disease Progression and Bone Lytic Disease. (**Oral presentation**, 2015 Annual Meeting of the Midwest Blood Club symposium Oct 9-11,2015, French lick, Indiana, US)

Xu LL, Himes E, Mohamad S, et al, A novel CD45+F4/80+ population within calvariae-derived osteoblasts regulates the osteoblast-mediated hematopoiesis enhancing activity through interactions with megakaryocytes. (**Poster presentation**, 2015 Annual Meeting of the Midwest Blood Club symposium Oct 9-11,2015, French lick, Indiana, US)

Xu LL, Machal C, Wu H, et al, CD166 Identifies Multiple Myeloma Cells That Preferentially Home to the Bone Marrow Microenvironment and Promote Disease Progression and Bone Lytic Disease. (**Oral presentation**, 2014 the American Society of Hematology annual meeting, Dec6-9, 2014, San Francisco, California, US)

Xu LL, Machal C, Wu H, et al, CD166 Directs Multiple Myeloma Cell Homing to the Bone Marrow Microenvironment and Promotes Disease Progression. (**Poster presentation**, 2014 Great Lakes International Imaging and Flow Cytometry Association Annual Meeting, Sep19-21, 2014, Oconomowoc, Wisconsin, US)

Xu LL, Machal C, Wu H, et al, Role Of CD166 In Multiple Myeloma Cell Homing To The Bone Marrow Microenvironment and Disease Progression. (**Poster presentation**, 2013 the American Society of Hematology annual meeting, Dec7-10, 2013, New Orleans, Louisiana, US)

Xu LL, Machal C, Wu H, et al, Role Of CD166 In Multiple Myeloma Cell Homing To The Bone Marrow Microenvironment. (**Poster presentation**, 2013 Annual Meeting of the Midwest Blood Club symposium Sep 19-20,2013, Cincinnati, Ohio, US)

Xu LL, Zheng GG, Ma CH, et al, The effect of mouse macrophages on the proliferation of mM-CSF-expressing Hematopoietic Malignant Cells (**Oral presentation**, the12th Chinese Society of Experimental Hematology (CESH) Annual Meeting Nov5-9, 2009 Chengdu, P.R. China)

Honors and Awards

American Society of Hematology Annual Meeting Abstract Achievement Award

Dec 2014

Great Lakes International Imaging and Flow Cytometry Association Annual Meeting

Travel Award

Sep 2014

Great Lakes International Imaging and Flow Cytometry Association Annual Meeting Best

Poster Award

Sep 2014

American Society of Hematology Annual Meeting Abstract Achievement Award

Dec 2013

Graduate Fellowship, Indiana University School of Medicine Biomedical Gateway (IBMG)

Aug 2010